

Fast Statistical Leverage Score Approximation in Kernel Ridge Regression

Yifan Chen

University of Illinois at Urbana-Champaign

YIFANC10@ILLINOIS.EDU

Yun Yang

University of Illinois at Urbana-Champaign

YY84@ILLINOIS.EDU

Abstract

Nyström approximation is a fast randomized method that rapidly solves kernel ridge regression (KRR) problems through sub-sampling the n -by- n empirical kernel matrix appearing in the objective function. However, the performance of such a sub-sampling method heavily relies on correctly estimating the statistical leverage scores for forming the sampling distribution, which can be as costly as solving the original KRR. In this work, we propose a linear time (modulo poly-log terms) algorithm to accurately approximate the statistical leverage scores in the stationary-kernel-based KRR with theoretical guarantees. Particularly, by analyzing the first-order condition of the KRR objective, we derive an analytic formula, which depends on both the input distribution and the spectral density of stationary kernels, for capturing the non-uniformity of the statistical leverage scores. Numerical experiments demonstrate that with the same prediction accuracy our method is orders of magnitude more efficient than existing methods in selecting the representative sub-samples in the Nyström approximation.

1. Introduction

The major computational bottleneck of kernel-based machine learning methods, such as kernel ridge regression (KRR) (Shawe-Taylor et al., 2004; Hastie et al., 2005), lies in the calculation of certain matrix inverse involving an n -by- n symmetric and positive semidefinite (PSD) empirical kernel matrix $K_n \in \mathbb{R}^{n \times n}$ over n inputs in the d -dimensional Euclidean space \mathbb{R}^d . For most common kernels, the empirical kernel matrix K_n is nearly singular with its effective rank being captured by the so-called *effective statistical dimension* (Alaoui and Mahoney, 2015; Yang et al., 2017b) d_{stat} that is problem-dependent and can be substantially smaller than the sample size n . For example, under the optimal choice of the regularization parameter, if the kernel function is a Matérn kernel with smoothness parameter $\nu > 0$, then the statistical dimension in the KRR is $d_{stat} = \mathcal{O}(n^{\frac{d}{2\nu+2d}})$ (Kanagawa et al., 2018).

1.1. Related Works

Due to this intrinsic low-rankness of K_n , several existing papers developed randomized algorithms, such as the Nyström method (Alaoui and Mahoney, 2015), randomized sketches (Yang et al., 2017b; Ahle et al., 2020), random Fourier features (Rahimi and Recht, 2008; Avron et al., 2017), and its improvement quadrature Fourier features (Mutny and Krause, 2018), for obtaining a rank $\tilde{\mathcal{O}}(d_{stat})$ ($\tilde{\mathcal{O}}(\cdot)$ means $\mathcal{O}(\cdot)$ modulo poly-log terms) approximation of K_n . In particular, sampling-based algorithms, such as the Nyström method, avoid

explicitly constructing the n -by- n matrix K_n , and only require $\tilde{\mathcal{O}}(nd_{stat})$ evaluations of the kernel function. This property is particularly appealing since both the time and space complexity can be reduced to even below the $\mathcal{O}(n^2)$ benchmark complexity of constructing and storing the empirical kernel matrix. From an algorithmic perspective, *statistical leverage scores*, as a measure of the structural non-uniformity of the inputs in forming K_n , can be used for constructing an importance sampling distribution that leads to high-quality low-rank approximations in the Nyström method. We refer the readers to some recent papers (Mahoney et al., 2011; Drineas et al., 2012) for more details.

However, the exact computation of the statistical leverage scores bears the same $\mathcal{O}(n^3)$ time complexity and $\mathcal{O}(n^2)$ space complexity (Mahoney et al., 2011) as inverting the n -by- n empirical kernel matrix. Researchers thus turn to the question of whether there is an efficient and accurate method of approximately computing the leverage scores. For example, some works (Alaoui and Mahoney, 2015; Rudi et al., 2015) borrowed the random projection idea (Drineas et al., 2012) in designing an approximation algorithm for computing the statistical leverage scores in the Nyström method in the context of KRR. Their algorithm has a worst case time complexity $\mathcal{O}(\frac{n^3}{d_{stat}^2})$ that may exceed the $\mathcal{O}(nd_{stat}^2)$ complexity in subsequent steps for small d_{stat} . As a refinement, Musco and Musco (2017) developed Recursive-RLS, a recursive version of the prior algorithm (Alaoui and Mahoney, 2015) with overall time complexity $\mathcal{O}(nd_{stat}^2)$ by alternating between updating the statistical leverage scores and drawing new subsamples based on the current scores. SQUEAK (Calandriello et al., 2017) adapts the algorithm to an online setting, attaining the same accuracy and having the same complexity order with only one pass over the data. BLESS (Rudi et al., 2018) adopts a path-following algorithm that further reduces the subsampling time complexity to $\mathcal{O}(\min(\frac{1}{\lambda}, n)d_{stat}^2 \log^2 \frac{1}{\lambda})$ where λ is the regularization parameter in the KRR. With the choice of $\lambda = \mathcal{O}(\frac{d_{stat}}{n})$ that leads to the optimal error rate, the complexity of BLESS would be $\tilde{\mathcal{O}}(nd_{stat})$.

1.2. Our Contribution

Most previous algorithms are algebraic methods by approximating matrix operations and apply to any positive semidefinite (PSD) kernel. In this work, we focus on stationary kernels and follow a completely different route of utilizing large sample properties of KRR to develop a new analytical approach for approximating the statistical leverage scores. Under a classical nonparametric setting, the new approach requires $\tilde{\mathcal{O}}(n)$ time and space complexity, and provably also attains the optimal statistical accuracy in the KRR. In a nutshell, rather than approximating the leverage scores by pre-constructing a low-rank approximation to K_n (Drineas et al., 2012), our method uses structural information contained in the kernel function and the underlying input distribution to infer how other inputs influence the statistical leverage score at a given location. In particular, we derive an explicit and computable formula,

$$\int_{\mathbb{R}^d} \frac{1}{p(x_i) + \lambda/m(s)} ds, \quad \forall i \in [n],$$

where $m(\cdot)$ is the spectral density function of the stationary kernel we use, and $p(x_i)$ is the density of the input x_i . This formula is applied to approximate the rescaled statistical

leverage score, which is proportional to the true statistical leverage score, at each observed point. We also provide the theoretical guarantees that the approximation formula has a vanishing relative error as $n \rightarrow \infty$.

Our development is based on the existing works (Silverman, 1984; Yang et al., 2017a) on the equivalent kernel representation of the KRR solution. The consequent theory sheds some light on the behaviour of leverage scores, and a simple application is the following rule of thumb: for the Matérn kernel with smoothness ν , the statistical leverage score at point x in \mathbb{R}^d is proportional to $\min\{1, (\lambda/p(x))^{1-d/(2\nu+d)}\}$, where the regularization parameter $\lambda = \Theta(d_{\text{stat}}/n)$. This scaling indeed matches the previous research on the asymptotic equivalent of the regularized Christoffel function (Pauwels et al., 2018), which has intrinsic connections with statistical leverage scores. We also show through numerical experiments that our method exhibits encouraging performance compared to other methods, which further improves the overall runtime of KRR.

2. Background and Problem Formulation

In this section, we set up the notation and briefly introduce the background. We begin with a short review on reproducing kernel Hilbert space (RKHS) and kernel ridge regression (KRR). After that, we invoke a useful and important formula that represents the norm of any RKHS induced by a stationary kernel via Fourier transforms and Parseval’s identity. Then we describe the class of Nyström -method-based approaches as our primary focus for approximately computing the KRR. Finally, we introduce the notation of equivalent kernel that plays important roles in both understanding the theoretical properties of the KRR and motivating our proposed method.

2.1. Reproducing kernel Hilbert space and kernel ridge regression

Reproducing kernel Hilbert space. Particularly, any RKHS is generated by a PSD kernel function $K : \mathcal{X} \times \mathcal{X} \rightarrow \mathbb{R}$, and there exists a correspondence between any RKHS (or its induced norm $\|\cdot\|_{\mathbb{H}}$) and its reproducing kernel (see the books (Berlinet and Thomas-Agnan, 2011; Wahba, 1990; Gu, 2013) for more details). Most widely used kernels are stationary, meaning that $K(x, y)$ depends on x and y only through their difference $(x - y)$. Due to this definition, we may abuse the notation $K(u)$ to mean $K(x, x + u)$ for any x . We will make this stationary kernel assumption throughout the paper. More specifically, we primarily focus on Matérn kernels, although the development can be straightforwardly extended to other stationary ones.

Kernel ridge regression. Consider a dataset $\mathcal{D}_n = \{(x_i, y_i)\}_{i=1}^n$ consisting of n pairs of points in $\mathcal{X} \times \mathcal{Y}$, where $\mathcal{X} \subseteq \mathbb{R}^d$ is the input (predictor) space and $\mathcal{Y} \subseteq \mathbb{R}$ the response space. To characterize the dependence of the response on the predictor, we assume the following standard nonparametric regression model as the underlying data generating model, $y_i = f^*(x_i) + \varepsilon_i$, $i = 1, 2, \dots, n$, where $f^* : \mathcal{X} \rightarrow \mathcal{Y}$ is the unknown regression function to be estimated, and the random noises $\{\varepsilon_i\}_{i=1}^n$ are i.i.d. $\mathcal{N}(0, \sigma^2)$, or any sub-Gaussian distribution with mean zero and variance σ^2 . Under the common regularity assumption that the true regression function f^* belongs to an RKHS \mathbb{H} , it is natural to estimate f^* by an estimator \hat{f} , which minimizes the sum of a least-squares goodness-of-fit term and a penalty term involving the squared norm $\|\cdot\|_{\mathbb{H}}$ associated with \mathbb{H} . This leads to the following

estimating procedure known as *kernel ridge regression* (KRR) (Shawe-Taylor et al., 2004; Hastie et al., 2005),

$$\hat{f} = \arg \min_{f \in \mathbb{H}} \left\{ \frac{1}{n} \sum_{i=1}^n (y_i - f(x_i))^2 + \lambda \|f\|_{\mathbb{H}}^2 \right\}. \quad (1)$$

The optimization problem (1) appears to be infinite-dimensional over a function space \mathbb{H} , while indeed its solution can be obtained by solving an n -dimensional quadratic program thanks to the representer theorem (Kimeldorf and Wahba, 1971). More precisely, for any two \mathcal{X} -valued vectors $a = (a_1, \dots, a_p)^T \in \mathcal{X}^p$ and $b = (b_1, \dots, b_q)^T \in \mathcal{X}^q$, we use the notation $K(a, b)$ to denote the p -by- q matrix whose (i, j) -th component is $K(a_i, b_j)$ for $i \in [p]$ and $j \in [q]$. Let $X_n = (x_1, \dots, x_n)^T \in \mathcal{X}^n$ and $Y_n = (y_1, \dots, y_n)^T \in \mathcal{Y}^n$. Under this notation, the solution \hat{f} takes the form as

$$\begin{aligned} \hat{f}(x) &:= K(x, X_n) (K_n + n\lambda I_n)^{-1} Y_n \\ &= \frac{1}{n} \sum_{i=1}^n G_\lambda(x, x_i) y_i, \end{aligned} \quad (2)$$

where $K_n := K(X_n, X_n)$ is the n -by- n empirical kernel matrix. Here, the weight function $G_\lambda : \mathcal{X} \times \mathcal{X} \rightarrow \mathbb{R}$ characterizes the impact of each observed pair (x_i, y_i) on $\hat{f}(x)$, and plays an important role in determining the optimal importance sampling weights in the Nyström method described. One key observation is that the weight function G_λ depends on the dataset \mathcal{D}_n only through the design points $\{x_i\}_{i=1}^n$ and the regularization parameter λ (which usually depends on the sample size n). This fact leads to the development of equivalent kernel approximation, as we will come back shortly in Section 2.4.

A final remark of the subsection is that solving for $\hat{\omega}$ requires time complexity $\mathcal{O}(n^3)$ of inverting an n -by- n matrix, which becomes formidable when n gets large. The practical demand of computationally scalable methods for implementing the KRR results in a large volume of literature on approximation algorithms, including our current work.

2.2. The relation between RKHS norm and Fourier transform

In this subsection, we describe a useful representation theorem that characterizes the RKHS of a stationary kernel function via the Fourier transform. Before formally introducing this theorem, we set up some notation. We use $L_p(\mathbb{R}^d) = \{f : \mathbb{R}^d \rightarrow \mathbb{R}, \int_{\mathbb{R}^d} |f(x)|^p dx < \infty\}$ to denote the space of all L_p integrable functions over \mathbb{R}^d for $p \geq 1$. For any function $f \in L_1(\mathbb{R}^d)$, we use $\mathcal{F}[f]$ to denote its Fourier transform defined by $\mathcal{F}[f](s) = \int_{\mathbb{R}^d} f(x) e^{-2\pi\sqrt{-1}x^T s} dx$, for all $s \in \mathbb{R}^d$, and $\mathcal{F}^{-1}[g]$ the inverse transform of a function g in the frequency domain as $\mathcal{F}^{-1}[g](x) = \int_{\mathbb{R}^d} g(s) e^{2\pi\sqrt{-1}x^T s} ds$, for all $x \in \mathbb{R}^d$. We use \bar{z} to denote the complex conjugate of any $z \in \mathbb{C}$, the space of complex numbers. The classical Bochner's theorem shows that the Fourier transform of any PSD and stationary kernel function is nonnegative.

The following theorem, which is not new but less well-known in the machine learning literature, provides a characterization of the RKHS with kernel K through its spectral density function. Similar statements can be found in two previous papers (Wendland 2004,

Thm 10.12 and Belkin 2018, Appendix A). For the sake of completeness, we also include a proof in Section A.2 in the appendix, which is motivated by Fukumizu (2008).

Theorem 1 (Fourier representation of RKHS) *Let function m be the spectral density of a PSD and stationary kernel K , and \mathbb{H} the associated RKHS. For any $f, g \in \mathbb{H}$, we have*

$$\begin{aligned} \|f\|_{\mathbb{H}}^2 &= \int_{\mathbb{R}^d} \frac{|\mathcal{F}[f](s)|^2}{m(s)} ds, \\ \text{and } \langle f, g \rangle_{\mathbb{H}} &= \int_{\mathbb{R}^d} \frac{\mathcal{F}[f](s) \cdot \overline{\mathcal{F}[g](s)}}{m(s)} ds. \end{aligned} \quad (3)$$

In particular, the RKHS can be represented by $\mathbb{H} = \{f : \|f\|_{\mathbb{H}}^2 = \int_{\mathbb{R}^d} |\mathcal{F}[f](s)|^2 / m(s) ds < \infty\}$.

2.3. Nyström methods with importance subsampling

From expression (2) of the KRR solution \hat{f} , the $\mathcal{O}(n^3)$ computational bottleneck comes from the inversion of the n -by- n matrix $(K_n + n\lambda I_n)$. When design points $\{x_i\}_{i=1}^n$ are distinct and sample size n is large, the empirical kernel matrix K_n often has a high condition number and is nearly low-rank. In particular, several recent studies (Alaoui and Mahoney, 2015; Yang et al., 2017b) show that both the computational and the statistical hardness of the KRR are captured by a quantity called the *statistical dimension* defined as

$$\begin{aligned} d_{\text{stat}} &:= \text{Tr}(K_n(K_n + n\lambda I_n)^{-1}) \\ &= \frac{1}{n} \sum_{i=1}^n G_{\lambda}(x_i, x_i), \end{aligned} \quad (4)$$

where $\text{Tr}(A)$ means the trace of a matrix A .

The statistical dimension d_{stat} approximately counts the number of eigenvalues of the rescaled kernel matrix $n^{-1}K_n$ whose values are above the threshold λ . Therefore, computing \hat{f} roughly amounts to solving an d_{stat} -dim quadratic program, and for most stationary kernels d_{stat} would be much smaller than n . For example, for a Matérn kernel with smoothness parameter ν being a positive half integer, $d_{\text{stat}} = \mathcal{O}(n^{\frac{d}{2\nu+2d}})$ (Tuo et al., 2020). Due to the intrinsic low-rankness of K_n , the so-called Nyström method, which replaces K_n with its low-rank approximation L_n , has been used for approximately solving the KRR (Gittens and Mahoney, 2016; Kumar et al., 2009; Williams and Seeger, 2001). Specially, the Nyström approximation of K_n is the matrix $L_n = K_n S (S^T K_n S)^{\dagger} S^T K_n$, where A^{\dagger} denotes the Moore-Penrose pseudoinverse of a matrix A , and $S \in \mathbb{R}^{n \times d_{\text{sub}}}$ is a zero-one subsampling matrix whose columns are a subset of the columns in I_n , indicating which d_{sub} observations have been selected. We use \hat{f}_{L_n} to denote the approximate KRR solution obtained by replacing K_n with L_n in expression (2).

Following the paper (Alaoui and Mahoney, 2015), we will refer to the diagonal elements of matrix $K_n(K_n + n\lambda I_n)^{-1}$ as the *statistical leverage scores* $\{\ell_i\}_{i=1}^n$ associated with the kernel matrix K_n . It is straightforward to verify from identity (2) that the i -th diagonal element of $K_n(K_n + n\lambda I_n)^{-1}$ is precisely $\frac{1}{n} G_{\lambda}(x_i, x_i)$, and thus we call $G_{\lambda}(x_i, x_i)$ the rescaled statistical leverage score.

The next result (Alaoui and Mahoney, 2015, Theorem 3) (after adapting to our notation) shows that if we use a randomized construction of S by sampling $d_{sub} = \mathcal{O}(d_{stat} \log(n))$ columns from I_n with a proper distribution $\{q_i\}_{i=1}^n$ over $[n]$ approximately proportional to the statistical leverage scores, the resulting approximate solution \hat{f}_{L_n} would attain the same statistical in-sample risk (up to a constant) as the original KRR solution \hat{f} . Here, we define the in-sample prediction risk for any regression function f as $R_n(f) = \|f - f^*\|_n^2 := n^{-1} \sum_{i=1}^n (f(x_i) - f^*(x_i))^2$.

Theorem 2 (Nyström approximation accuracy) *Fix $\rho \in (0, 1/2)$. Let L_n be the Nyström approximation of K_n with S being formed by choosing d columns randomly with replacement from the columns of the identity matrix I_n according to a probability distribution $\{q_i\}_{i=1}^n$. Suppose there exists some $\beta \in (0, 1]$ such that $q_i \geq \beta G_\lambda(x_i, x_i) / \sum_{i=1}^n G_\lambda(x_i, x_i)$, and*

$$d_{sub} \geq C_1 \frac{d_{stat}}{\beta} \log\left(\frac{n}{\rho}\right) \quad \text{and} \quad \lambda \geq \frac{C_2}{\min_i G_\lambda(x_i, x_i)},$$

where d_{stat} is defined in (4). Then it holds with probability at least $1 - 2\rho$ that $R_n(\hat{f}_{L_n}) \leq C_3 R_n(\hat{f})$. Here C_i , $i = 1, 2, 3$, are absolute constants.

This theorem indicates that the problem of approximately solving the KRR reduces to that of approximately estimating the statistical leverage scores $\{\ell_i\}_{i=1}^n$. Directly computing these leverage scores using SVD requires inverting an n -by- n matrix and is as costly as solving the original KRR optimization (2). Finding purely numerical methods for approximating these leverage scores can also be quite challenging. For example, the approximation algorithm used in the paper (Alaoui and Mahoney, 2015) has $\mathcal{O}\left(\frac{n^3}{d_{stat}^2}\right)$ time complexity, which significantly exceeds the $\mathcal{O}(nd_{stat}^2)$ complexity for forming L_n and solving for \hat{f}_{L_n} in the Nyström approximation when $d_{stat} \ll \sqrt{n}$ (which holds for any Matérn kernel).

2.4. Equivalent Kernel

Our method is initially motivated by a notion, *equivalent kernel*, which was first introduced by Silverman (1984). The author showed that in the context of smoothing spline regression, as sample size n goes to infinity the weight function $G_\lambda(\cdot, \cdot)$ after a proper rescaling approaches a limiting kernel function, called the equivalent kernel. A recent work (Yang et al., 2017a, Theorem 2.1) extends the context from smoothing spline regression to general kernel ridge regression. They proved that for a general kernel K , under the stochastic assumption that design points $\{x_i\}_{i=1}^n$ are i.i.d. distributed according to a common distribution over \mathcal{X} , there exists some equivalent kernel $\bar{K}_\lambda : \mathcal{X} \times \mathcal{X} \rightarrow \mathbb{R}$, such that the KRR estimator is asymptotically the same as a simple kernel type estimator with kernel function \bar{K}_λ , that is, under a suitable choice of diminishing regularization parameter λ , the following approximation error bound holds with probability tending to one as $n \rightarrow \infty$,

$$\sup_{x \in \mathcal{X}} \left| \hat{f}(x) - \frac{1}{n} \sum_{i=1}^n \bar{K}_\lambda(x, x_i) y_i \right| \leq \gamma_n \sqrt{\lambda}, \quad (5)$$

where $\gamma_n \rightarrow 0$ as $n \rightarrow \infty$ and $\sqrt{\lambda}$ matches the maximal magnitude of the estimation error $\sup_{x \in \mathcal{X}} |\hat{f}(x) - f^*(x)|$. Formula (5) predicts a theoretical limit of the statistical leverage score ℓ_i as $\bar{K}_\lambda(x_i, x_i)$ that is *independent* of the design points other than x_i . In other words, the KRR estimator can be expressed as a linear combination of y_i 's, whose coefficients only depend on the corresponding design point x_i . Besides, under mild conditions (Yang et al., 2017a) on the design distribution, these coefficients admit a limit in probability (that can be characterized via an “equivalent kernel” function) as $n \rightarrow \infty$. The theoretical result motivates us to seek a computationally efficient method for the leverage scores through approximating these $\bar{K}_\lambda(x_i, x_i)$'s.

3. Leverage Score Approximation via Spectral Analysis

We now turn to the main results of this work. At a high level, we propose our method and give a sketch of the derivation via Fourier transform. We also provide the analysis of the corresponding time complexity and consider some stationary kernels to which our method would be applied. Eventually, we prove that, by taking Matérn kernels as an example, our method would attain an optimal prediction risk in the KRR.

3.1. The proposed algorithm and a heuristic derivation

Under the notation above, we formally propose the explicit formula of our approximation method as

$$\tilde{K}_\lambda(x_i, x_i) = \int_{\mathbb{R}^d} \frac{1}{p(x_i) + \lambda/m(s)} ds, \quad (6)$$

where $p(x_i)$ is the density of x_i defined in Section 1.2. With Eqn (6), we would use Algorithm 3.1 below to approximate $G_\lambda(x_i, x_i)$ for some fixed point $x_i \in \mathbb{R}^d$.

Input: the input samples X_n and the spectral density $m(\cdot)$ of the stationary kernel used

Output: A discrete sampling distribution $\{q_i\}_{i=1}^n$

Initialize the sampling distribution $q_i = 0, \forall i = 1, \dots, n$ Estimate the density p_i of the samples $x_i, \forall i = 1, \dots, n$ **for** $i=1:n$ **do**

 | Compute the integration (6) with p_i , and assign the value to q_i

end

Denote $Q = \sum_{i=1}^n q_i$ Update q_i as $q_i/Q, \forall i = 1, \dots, n$

Algorithm 1: Estimation of the leverage scores

To derive the formula (6), by setting $y_i = n, y_j = 0$ (for any $j \neq i$), we transform the objective value in the KRR optimization problem (1) to the following functional:

$$\begin{aligned} A_{n,x_i}(f) &= \frac{1}{2n} \sum_{j=1}^n f(x_j)^2 + \frac{1}{2} \lambda \|f\|_{\mathcal{H}}^2 - f(x_i) \\ &= \frac{1}{2} \int_{\mathbb{R}^d} f(x)^2 dF_n(x) + \frac{1}{2} \lambda \|f\|_{\mathcal{H}}^2 - f(x_i), \end{aligned}$$

for any function $f \in \mathbb{H}$, where F_n denotes the empirical distribution of $\{x_i\}_{i=1}^n$ and the integral is the Riemann–Stieltjes integral. The minimizer of $A_{n,x_i}(f)$ would simply be $\hat{f}(\cdot) =$

$\frac{1}{n} \sum_{j=1}^n G_\lambda(\cdot, x_j) y_j = G_\lambda(\cdot, x_i)$, due to the independence of G_λ from $\{y_i\}_{i=1}^n$. Therefore, it suffices to analyze and understand this functional A_{n,x_i} for any $x_i \in \mathcal{X}$. Now we assume that there exists a nice cdf F over \mathcal{X} that admits a Lipschitz continuous density function denoted by p , so that the sup-norm $\tau(n) = \|F_n - F\|_\infty := \sup_{x \in \mathcal{X}} |F_n(x) - F(x)|$ is small. We further remark here that in the most common case, $\{x_i\}_{i=1}^n$ are i.i.d. from pdf p , and then $\tau(n) \leq C\sqrt{\log n/n}$ holds with high probability due to the Glivenko-Cantelli theorem (Van Der Vaart and Wellner, 1996). Since A_{n,x_i} is convex, finding its optimum amounts to finding the unique root of its functional derivative (such as the Gateaux derivative), which is a linear operator $DA_{n,x_i}(f) : \mathbb{H} \rightarrow \mathbb{H}$ defined at each $f \in \mathbb{H}$ as

$$DA_{n,x_i}(f)(u) = \int_{\mathbb{R}^d} f(x) u(x) dF_n(x) + \lambda \langle f, u \rangle_{\mathbb{H}} - u(x_i), \quad \text{for any } u \in \mathbb{H}.$$

Since F_n can be well-approximated by F under the assumption $\tau(n) \rightarrow 0$ and the solution $G_\lambda(\cdot, x_i)$ is expected to approach to a Dirac delta function centered at x_i as $n \rightarrow \infty$ (which will be formalized in Section C in the appendix), the above derivative can thus be approximated by a simpler population-level functional

$$DA_{x_i}(f)(u) = p(x_i) \int_{\mathbb{R}^d} f(x) u(x) dx + \lambda \langle f, u \rangle_{\mathbb{H}} - u(x_i), \quad \text{for any } u \in \mathbb{H},$$

where we replace the differential $dF_n(x)$ with its local approximate $p(x_i)dx$. This new operator admits a simpler form in the frequency domain thanks to Parseval's theorem (cf. Theorem 7 and Lemma 8 in the appendix),

$$DA_{x_i}(f)(u) = \int_{-\infty}^{\infty} \left(p(x_i) \mathcal{F}[f](s) + \frac{\lambda}{m(s)} \mathcal{F}[f](s) - \exp \{ -2\pi\sqrt{-1}x_i s \} \right) \overline{\mathcal{F}[u](s)} ds.$$

Therefore, the unique root of $DA_{x_i}(\cdot)$, denoted by $\tilde{K}_\lambda(\cdot, x_i)$, can be obtained by equating the function inside the big parenthesis in the preceding display to zero, which is the inverse Fourier transform of

$$\frac{\exp \{ -2\pi\sqrt{-1} \langle x_i, s \rangle \}}{p(x_i) + \lambda/m(s)}, \quad s \in \mathbb{R}^d, \quad (7)$$

or $\tilde{K}_\lambda(\cdot, x_i) = \mathcal{F}^{-1}[(p(x_i) + \lambda/m(s))^{-1}](\cdot - x_i)$ due to the translation property of the Fourier transform. Replacing x_i with the i -th design point x_i leads to the following quantity

$$\tilde{K}_\lambda(x_i, x_i) = \int_{\mathbb{R}^d} \frac{1}{p(x_i) + \lambda/m(s)} ds,$$

due to the inverse Fourier transform formula. We show its applications to Matérn kernels as follows.

Example (Matérn kernels): Matérn family (Matérn, 2013) is a class of isotropic kernels widely used in spatial statistics. The kernel function is expressed as $C_\nu(x, y) = C_\nu(x - y) = \frac{2^{1-\nu}}{\Gamma(\nu)}(a\|x - y\|)^\nu B_\nu(a\|x - y\|)$, where B_ν is a modified Bessel function of the second kind, ν is a smoothness parameter (usually half integers), and $a > 0$ a scale parameter. Here we slightly abused the notation since C_ν is stationary. An important fact about the Matérn kernel C_ν is that its associated RKHS is the $(\nu + d/2)$ -th order Sobolev space (we can verify it by plugging the following Fourier transform $m_\alpha(\cdot)$ into Theorem 1). The notation $\alpha = \nu + d/2$ is hence used to denote the underlying smoothness level associated with kernel $K_\alpha := C_{\alpha-d/2}$, and the rescaled leverage approximation \tilde{K}_λ associated with K_α satisfies $\tilde{K}_\lambda(\cdot, x_i) = \mathcal{F}^{-1}\left[\left(p(x_i) + \lambda D_\alpha^{-1}(a^2 + \|s\|^2)^\alpha\right)^{-1}\right](\cdot - x_i)$, where $a = \sqrt{2\nu}$, $D_\alpha = \Gamma(\alpha)a^{2\alpha-1}\pi^{-d/2}/\Gamma(2\alpha - 1)$. For general density function p , the integral formula (6) with $m = m_\alpha$ provides a rule of thumb on how the statistical leverage score depends on the local input density as $\ell_i \propto \min\{1, (\lambda/p(x_i))^{1-d/(2\alpha)}\}$, which implies a relatively large value over those under-sampled regions with small $p(x_i)$.

3.2. Computational complexity

To give the complexity analysis, we first stress that in our theoretical development the dimension d is either fixed or at most slowly (e.g. logarithmically) increases with the sample size n . Beyond this setting, at least theoretically, the smallest subsampling size (via statistical dimension d_{stat} , which is $\mathcal{O}((\log n)^{\frac{d}{2}})$ even under a Gaussian kernel) becomes comparable to n , making subsampling meaningless due to the curse of dimensionality. In addition, classical nonparametric literature (Silverman, 1984; Yang et al., 2017a; van der Vaart et al., 2009) suggests that a dimension d of order $o(\log n)$ is necessary to make any estimator consistent.

With the requirement on d above, we claim $\tilde{K}_\lambda(x_i, x_i)$ can be efficiently computed in $\tilde{\mathcal{O}}(n)$ time. Specifically, the overall complexity includes two parts, numerical integration, and density estimation. A key observation here is that for both parts the error rates are only required to be sub-optimal, and $o(1)$ relative error suffices to guarantee the optimality of the error rate in the KRR. With such a high tolerance of error, the two parts above could both be implemented in $\tilde{\mathcal{O}}(n)$ time as claimed (see Section D, E in the appendix for more details).

In particular, the overall complexity can be made at most polynomial in the dimension d . For the integration part, we can avoid the exponential dependence on d by applying a polar coordinate transformation to reduce the multivariate integral (6) to a univariate integral (c.f. Section D in the appendix). For density estimation, some advanced methods are able to generate n density estimates at sample design points in $\mathcal{O}(nd \log n)$ time with relative approximation error (difference between accurate KDE and approximation methods) of magnitude $\mathcal{O}((\log n)^{-1/2})$ (such as ASKIT (March et al., 2015, Eqn (3.3)), HBE (Charikar and Siminelakis, 2017, Theorem 12), and modified HBE (Backurs et al., 2019, Theorem 1)). (Those methods only aim to approximate the original KDE, and hence have no requirements on the density but the kernel used in KDE. The exact set of assumptions for modified HBE are provided in Section E.1 in the appendix.) In practice, when the KRR problem of interest is not high dimensional ($d = \omega(1)$), we are even able to efficiently estimate the density with

the optimal error rate in $\mathcal{O}(n(\log n)^d)$ time, by some classical approaches (such as KD-tree methods (Ivezic et al., 2014), fast multipole methods (Greengard and Rokhlin, 1997), and fast Gauss transforms (Greengard and Strain, 1991)), which are empirically be even faster than the advanced KDE methods above.

As a closing of this subsection, we leave a comment regarding Gaussian kernels. It seems Gaussian kernels have a low statistical dimension $d_{stat} = \mathcal{O}((\log n)^{d/2})$, which may allow previous leverage approximation methods, such as BLESS, to have a time complexity comparable to our method. We point out here the complete expression for the scale of d_{stat} should be $\mathcal{O}(\sigma^{-d}(\log(n\sigma^{2d}))^{d/2})$ (Yang et al., 2017b), where σ is the bandwidth of the Gaussian kernel used. It implies the statistical dimension of Gaussian Kernels would actually be heavily impacted by the bandwidth σ . However, as we hope to attain the optimal error rate in KRR, we need to decrease the bandwidth σ of Gaussian kernels to $\mathcal{O}(n^{-c})$ ($c \in (0, \frac{1}{2d})$) to significantly enrich the associated RKHS (van der Vaart et al., 2009). As a trade-off, the magnitude of d_{stat} would simultaneously be increased to a polynomial of n , which is comparable to the scale of d_{stat} using a proper Matérn kernel. Therefore, generally Gaussian kernels cannot enable the previous leverage approximation methods to enjoy the $\tilde{\mathcal{O}}(n)$ complexity.

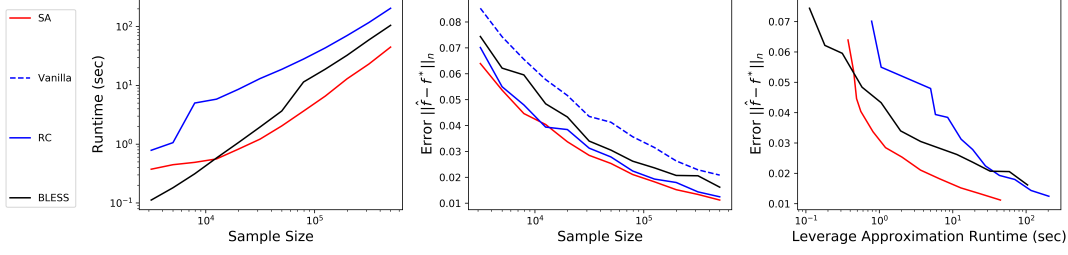


Figure 1: Run time vs. error tradeoff.

3.3. Theoretical results

We focus on the Matérn kernel K_α (proof for other stationary kernels can be developed similarly) and define the effective bandwidth parameter, an important auxiliary parameter analogous to the bandwidth of a Gaussian kernel, as $h := \lambda^{1/(2\alpha)}$, which indicates the smoothness of the functions in the corresponding RKHS. When λ is set to obtain the minimax-optimal KRR estimator \hat{f} , the scale of h would therefore be $\Theta(n^{-1/(2\alpha+d)})$. Our first result provides an explicit error bound on $|G_\lambda(\cdot, x_i) - \tilde{K}_\lambda(\cdot, x_i)|$ in a neighborhood of x_i . Particularly, Lemma 12 in the appendix shows that the equivalent kernel $\tilde{K}_\lambda(\cdot, x_i)$ resembles a Dirac delta function centered at x_i with radius $\mathcal{O}(h)$, so it suffices to characterize its difference with $G_\lambda(\cdot, x_i)$ in the local neighborhood. The regularity assumptions of our results are listed as follows:

Assumption 3 *There exists a distribution F whose density function p is Lipschitz continuous, so that $\tau(n) = \|F_n - F\|_\infty \leq C_0 h^2$ for some constant $C_0 > 0$.*

Assumption 4 *The density function p is strictly positive at the points $x_i, i = 1, \dots, n$. Besides, for each i , there exists some $\delta(x_i)$, such that $p(x) \geq \frac{p(x_i)}{2}$ for all $x \in B(x_i, \delta(x_i)) := \{x; \|x - x_i\| < \delta(x_i)\}$, and $\delta(x_i) \geq Ch \log(\frac{1}{h}), \forall i \in [n]$ for some sufficiently large constant C independent of (x_i, h, n) .*

Assumption 3 needs the empirical distribution F_n to be well-approximated by a smooth cdf F (c.f. Section 3.1). Assumption 4 requires x_i to be a proper interior point of the support of p , or at least $\Theta(h \log(\frac{1}{h}))$ far away from the zero density region. These two assumptions are mild. Assumption 1 is indeed a generalized version of a common assumption “ x_i ’s are drawn iid from a distribution F with Lipschitz density p ”, while also compatible with fixed design setting. Assumption 1 would automatically be satisfied when the quoted assumption holds, with $\tau(n) = \mathcal{O}((d/n)^{1/2})$ guaranteed by multivariate Glivenko-Cantelli theorem (p. 828 Shorack and Wellner, 2009, Theorem 1). Another remark about Assumption 3 is that the Lipschitz continuity of the density p is enough for KDE to produce consistent estimation with mean squared error $\mathcal{O}(n^{-\frac{2}{d+2}})$ (Walter et al., 1979), which is even dominated by the approximation error of the KDE approximation methods mentioned above. (Thus now we can conclude the KDE methods above with $\mathcal{O}(nd \log n)$ time complexity could provide sufficient accuracy.) For Assumption 2, as long as $p(x_i) > 0$ and p is continuous, it always holds in the large scale setting as $n \rightarrow \infty$ since $h \log(\frac{1}{h}) \rightarrow 0$ as $h \rightarrow 0$. Moreover, we only need to verify it for the observed design points $\{x_i\}_{i=1}^n$ in conjunction with Theorem 2, and by definition $p(\cdot)$ is automatically positive at these observed points.

Theorem 5 (Leverage score approximation) *If Assumptions 3 and 4 hold, then for any $i \in [n]$*

$$\begin{aligned} \sup_{x \in B(x_i, \delta(x_i))} |G_\lambda(x, x_i) - \tilde{K}_\lambda(x, x_i)| \\ \leq C_{x_i} h^{-d} (\tau(n) h^{-d} + h). \end{aligned}$$

In particular, the relative error of approximating $G_\lambda(x_i, x_i)$ by the integral (6) satisfies

$$\frac{|G_\lambda(x_i, x_i) - \tilde{K}_\lambda(x_i, x_i)|}{|G_\lambda(x_i, x_i)|} \leq C'_{x_i} (\tau(n) h^{-d} + h).$$

Here we may choose $C_{x_i} = C \max\{1, p^{-1/2}(x_i)\}$ and $C'_{x_i} = C \max\{1, p^{1/2-d/(2\alpha)}(x_i)\} \sqrt{p(x_i)}$ for some constant C independent of (x_i, h, n) .

The proof of this theorem relies on a novel Sobolev interpolation inequality that bounds the localized sup-norm via the RKHS norm $\|\cdot\|_{\mathbb{H}}$ plus a localized L_2 norm. We remark that the rescaled leverage score $G_\lambda(x_i, x_i)$ and our approximation $\tilde{K}_\lambda(x_i, x_i)$ would both increase to infinity as $n \rightarrow \infty$, and the upper bound for the difference between them would also diverge as shown in the first inequality above; however, the relative error, the quantity of our interest, would shrink. Combining the above with Theorem 2, we can show our approximation leads to an optimal prediction risk in the approximated KRR.

Table 1: Statistical Leverage Score Approximation Accuracy

Method	RQC			HTRU2			CCPP		
	Time	\bar{r}	$5^{th}/95^{th}$	Time	\bar{r}	$5^{th}/95^{th}$	Time	\bar{r}	$5^{th}/95^{th}$
SA	0.40	1.01	0.87/1.13	2.23	1.04	0.77/1.26	0.48	1.00	0.79/1.21
Vanilla	-	1.06	0.64/1.40	-	1.13	0.53/1.63	-	1.04	0.72/1.33
RC	6.97	1.03	0.75/1.33	2.15	1.05	0.75/1.27	9.21	1.02	0.82/1.24
Bless	3.83	1.03	0.74/1.33	1.63	1.07	0.67/1.32	5.25	1.02	0.81/1.24

Theorem 6 (Nyström approximation) *Suppose Assumptions 3, 4 hold for each $x_i, i = 1, \dots, n$. Under the same setting and conditions Theorem 2, if the importance sampling weights are chosen as $q_i = \tilde{K}_\lambda(x_i, x_i) / \sum_{i=1}^n \tilde{K}_\lambda(x_i, x_i)$, we have $R_n(\hat{f}_{L_n}) \leq C_3 R_n(\hat{f})$ with probability at least $1 - 2\rho$.*

4. Experiments

In this section, we evaluate our leverage score approximation method on both synthetic and real datasets. The algorithms below are implemented in unoptimized Python code, run with one core of a server CPU (Intel Xeon-Gold 6248 @ 2.50GHZ) on Red Hat 4.8. Specifically, we perform the numerical integration and density estimation as described in Section D and E in the appendix. Due to the limited space, the complete settings of the experiments below and more supplementary results can be found in Section B in the appendix.

4.1. Performance in kernel ridge regression

We compare the in-sample prediction error of Nyström methods in KRR, as well as the corresponding leverage approximation time among all the competing algorithms: uniform sampling (hereinafter referred to as “Vanilla”), Recursive-RLS (RC), (Musco and Musco, 2017), Bottom-up Leverage Scores Sampling (BLESS) (Rudi et al., 2018) and our proposed spectral-analysis-based method (SA). (The Monte Carlo approximation for the regularized Christoffel function (Pauwels et al., 2018) in practice reduces to directly computing leverage scores and is thus omitted.) In the experiment, we generate design points $\{x_i\}_{i=1}^n$ with $n \in [2000, 500000]$ from a 3-D bimodal distribution (see Section B in the appendix for the definition). We use squared in-sample estimation error $\|\hat{f} - f^*\|_n^2$ as the evaluation metric. All the results reported in Figure 1 are averaged over 30 replicates. We remark that in the left or the right subplot there is no curve for “Vanilla” method, as this method assumes the leverage scores are uniform and thus takes no time to approximate.

In Figure 1, we can observe “Vanilla” fails to capture the information of the entire design distribution as expected, as with high probability, only few data points from the small mode would be sampled. For RC, BLESS, and our method, although they are all able to capture the non-uniformity, our method has the best runtime versus error trade-off, especially when n is large. Particularly, when $n = 5 \times 10^5$ our method takes 35.8s to approximate the leverage scores, while RC and BLESS respectively take a higher cost—around 94.3s and 167s—due to their higher complexities.

4.2. Statistical leverage scores accuracy

We empirically validate that the approximation $\tilde{K}_\lambda(x_i, x_i)$ approaches the rescaled statistical leverage score $G_\lambda(x_i, x_i)$ as guaranteed by our theory. In particular, we compare the true rescaled leverage and our approximation for samples from one-dimensional (for the ease of visualization) $\text{Unif}[0, 1]$, $\text{Beta}(15, 2)$, and a bimodal distribution.

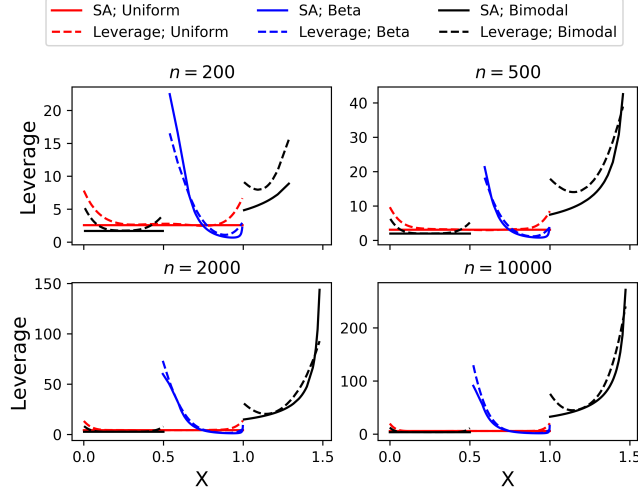


Figure 2: Statistical Leverage Score Approximation

In Figure 2, dotted curves correspond to the rescaled leverage scores, while solid curves correspond to the equivalent kernel approximations. We can observe our method provides good approximations to the rescaled leverage scores across all settings. In particular, $\text{Unif}[0, 1]$ is the easiest case (red curves) due to its flat density, which meets Assumption 3 and 4 for almost all design points; while for points with low density, such as those in the smaller cluster of the bimodal distribution and close to the boundary of $\text{Beta}(15, 2)$, the absolute error tends to be large, due to the leading constant C_{x_i} in the error bound in Theorem 5. Moreover, the relative approximation error has a clear tendency to decrease as the sample size increases, which is consistent with our theory.

We also quantitatively study the accuracy of the leverage scores obtained by different methods in the last section. Each algorithm is tested on `RadiusQueriesCount` (Savva et al., 2018; Anagnostopoulos et al., 2018) (denoted by RQC), `HTRU2` (Lyon et al., 2016), and `CCPP` (Tüfekci, 2014; Kaya and Tüfekci, 2012), the datasets downloaded from the UCI ML Repository (Dua and Graff, 2017). Those datasets contain 10000, 17898, and 9568 data points respectively, which are at the limit of our computational feasibility (it requires $\mathcal{O}(n^3)$ time and $\mathcal{O}(n^2)$ space to exactly compute leverage scores). We begin by normalizing the datasets before constructing the kernel matrix using Matérn kernel ($\nu = 0.5$). Each method is then used to approximate the leverage scores $\{\tilde{\ell}_i\}_1^n$. The sampling probability \tilde{q}_i is obtained as $\tilde{\ell}_i / (\sum_1^n \tilde{\ell}_i)$ (also denoting $q_i = \ell_i / (\sum_1^n \ell_i)$). The accuracy of each method

is measured by the average of the ratios $\{r_i := \tilde{q}_i/q_i\}_1^n$ (R-ACC). The complete setting for this experiment can be found in Section B in the appendix.

In Table 1 we report the runtime, mean R-ACC \bar{r} , and the 5th / 95th quantile of R-ACC, averaged over 10 replicates. We notice that, regarding the leverage approximation, our method provides the most accurate leverage approximation (in terms of mean R-ACC), and is more efficient than other methods on the benchmark datasets, which matches the complexity analysis.

4.3. Additional empirical results

In Section E.1 in the appendix, we further provide some empirical results to compare different approximation methods for increasing input dimension d . In short, under the certain setting the prediction accuracy of all the methods will greatly deteriorate due to the curse of dimensionality, and the classical Nyström method with uniform sampling will be preferred as leverage-based sampling cannot bring many benefits to the statistical performance.

5. Conclusion and future work

We propose a new method to estimate the leverage scores in kernel ridge regression for fast Nyström approximation when a stationary kernel is used. Theoretical results are also provided to guarantee the high accuracy of our estimation. In particular, we show that under the mild conditions the leverage scores induced by a Matérn empirical kernel matrix can be estimated in $\tilde{O}(n)$ time, where n is the size of input samples.

A direct further development of our current work is the extension of our theory to other stationary kernels, such as Gaussian kernels and exponential kernels. Other related questions include the performance guarantees when the new leverage estimation method is applied to kernel methods for other machine learning problems, for example, kernel k -means and kernel PCA. It will also be interesting to follow the heuristic procedure in our method to analyze other kernel models involving linear smoothers, and seek the possibility to accelerate those models. The results in this work also shed new light on the relevance of the “equivalent kernel” (Yang et al., 2017a) and the regularized Christoffel function (Pauwels et al., 2018) mentioned in Section 1.2.

Acknowledgments

This work is supported by NSF grant DMS-1810831.

References

- Robert A Adams and John JF Fournier. *Sobolev spaces*, volume 140. Elsevier, 2003.
- Thomas D Ahle, Michael Kapralov, Jakob BT Knudsen, Rasmus Pagh, Ameya Velingker, David P Woodruff, and Amir Zandieh. Oblivious sketching of high-degree polynomial kernels. In *Proceedings of the Fourteenth Annual ACM-SIAM Symposium on Discrete Algorithms*, pages 141–160. SIAM, 2020.

- Ahmed Alaoui and Michael W Mahoney. Fast randomized kernel ridge regression with statistical guarantees. In *Advances in Neural Information Processing Systems*, pages 775–783, 2015.
- Christos Anagnostopoulos, Fotis Savva, and Peter Triantafillou. Scalable aggregation predictive analytics. *Applied Intelligence*, 48(9):2546–2567, 2018.
- Haim Avron, Michael Kapralov, Cameron Musco, Christopher Musco, Ameya Velingker, and Amir Zandieh. Random fourier features for kernel ridge regression: Approximation bounds and statistical guarantees. In *Proceedings of the 34th International Conference on Machine Learning-Volume 70*, pages 253–262. JMLR. org, 2017.
- Arturs Backurs, Piotr Indyk, and Tal Wagner. Space and time efficient kernel density estimation in high dimensions. In *Advances in Neural Information Processing Systems*, pages 15773–15782, 2019.
- Mikhail Belkin. Approximation beats concentration? an approximation view on inference with smooth radial kernels. In *Conference On Learning Theory*, pages 1348–1361. PMLR, 2018.
- Alain Berlinet and Christine Thomas-Agnan. *Reproducing kernel Hilbert spaces in probability and statistics*. Springer Science & Business Media, 2011.
- Haïm Brezis and Petru Mironescu. Gagliardo–nirenberg inequalities and non-inequalities: The full story. In *Annales de l’Institut Henri Poincaré C, Analyse non linéaire*, volume 35, pages 1355–1376. Elsevier, 2018.
- Daniele Calandriello, Alessandro Lazaric, and Michal Valko. Distributed adaptive sampling for kernel matrix approximation. In *Artificial Intelligence and Statistics*, pages 1421–1429, 2017.
- Moses Charikar and Paris Siminelakis. Hashing-based-estimators for kernel density in high dimensions. In *2017 IEEE 58th Annual Symposium on Foundations of Computer Science (FOCS)*, pages 1032–1043. IEEE, 2017.
- Richard E Crandall. Note on fast polylogarithm computation. 2006.
- Lokenath Debnath, Piotr Mikusinski, et al. *Introduction to Hilbert spaces with applications*. Academic press, 2005.
- Petros Drineas, Malik Magdon-Ismail, Michael W Mahoney, and David P Woodruff. Fast approximation of matrix coherence and statistical leverage. *Journal of Machine Learning Research*, 13(Dec):3475–3506, 2012.
- Dheeru Dua and Casey Graff. UCI machine learning repository, 2017. URL <http://archive.ics.uci.edu/ml>.
- Kenji Fukumizu. Elements of positive definite kernel and reproducing kernel hilbert space, 2008.

- Alex Gittens and Michael W Mahoney. Revisiting the nyström method for improved large-scale machine learning. *The Journal of Machine Learning Research*, 17(1):3977–4041, 2016.
- Leslie Greengard and Vladimir Rokhlin. A fast algorithm for particle simulations. *Journal of Computational Physics*, 135(2):280–292, 1997.
- Leslie Greengard and John Strain. The fast gauss transform. *SIAM Journal on Scientific and Statistical Computing*, 12(1):79–94, 1991.
- Chong Gu. *Smoothing spline ANOVA models*, volume 297. Springer Science & Business Media, 2013.
- Trevor Hastie, Robert Tibshirani, Jerome Friedman, and James Franklin. The elements of statistical learning: data mining, inference and prediction. *The Mathematical Intelligencer*, 27(2):83–85, 2005.
- Zeljko Ivezić, Andrew J Connolly, Jacob T VanderPlas, and Alexander Gray. *Statistics, Data Mining, and Machine Learning in Astronomy: A Practical Python Guide for the Analysis of Survey Data*. Princeton University Press, 2014.
- Fredrik Johansson. Rigorous high-precision computation of the hurwitz zeta function and its derivatives. *Numerical Algorithms*, 69(2):253–270, 2015.
- Motonobu Kanagawa, Philipp Hennig, Dino Sejdinovic, and Bharath K Sriperumbudur. Gaussian processes and kernel methods: A review on connections and equivalences. *arXiv preprint arXiv:1807.02582*, 2018.
- Heysem Kaya and Pinar Tüfekci. Local and global learning methods for predicting power of a combined gas & steam turbine. In *International Conference on Emerging Trends in Computer and Electronics Engineering*, 03 2012.
- George Kimeldorf and Grace Wahba. Some results on tchebycheffian spline functions. *Journal of mathematical analysis and applications*, 33(1):82–95, 1971.
- William Kleiber and Douglas W Nychka. Spatial statistics. 2015.
- Sanjiv Kumar, Mehryar Mohri, and Ameet Talwalkar. Sampling techniques for the nystrom method. In *Artificial Intelligence and Statistics*, pages 304–311, 2009.
- Robert J Lyon, BW Stappers, Sally Cooper, JM Brooke, and JD Knowles. Fifty years of pulsar candidate selection: from simple filters to a new principled real-time classification approach. *Monthly Notices of the Royal Astronomical Society*, 459(1):1104–1123, 2016.
- Michael W Mahoney et al. Randomized algorithms for matrices and data. *Foundations and Trends® in Machine Learning*, 3(2):123–224, 2011.
- William B March, Bo Xiao, and George Biros. Askit: Approximate skeletonization kernel-independent treecode in high dimensions. *SIAM Journal on Scientific Computing*, 37(2):A1089–A1110, 2015.

- Bertil Matérn. *Spatial variation*, volume 36. Springer Science & Business Media, 2013.
- Cameron Musco and Christopher Musco. Recursive sampling for the nystrom method. In *Advances in Neural Information Processing Systems*, pages 3833–3845, 2017.
- Mojmir Mutny and Andreas Krause. Efficient high dimensional bayesian optimization with additivity and quadrature fourier features. In *Advances in Neural Information Processing Systems*, pages 9005–9016, 2018.
- Edouard Pauwels, Francis Bach, and Jean-Philippe Vert. Relating leverage scores and density using regularized christoffel functions. In *Advances in Neural Information Processing Systems*, pages 1663–1672, 2018.
- Robert Piessens, Elise de Doncker-Kapenga, Christoph W Überhuber, and David K Kahaner. *Quadpack: a subroutine package for automatic integration*, volume 1. Springer Science & Business Media, 2012.
- Ali Rahimi and Benjamin Recht. Random features for large-scale kernel machines. In *Advances in neural information processing systems*, pages 1177–1184, 2008.
- Carl Edward Rasmussen. Gaussian processes in machine learning. In *Summer School on Machine Learning*, pages 63–71. Springer, 2003.
- Alessandro Rudi, Raffaello Camoriano, and Lorenzo Rosasco. Less is more: Nyström computational regularization. In *Advances in Neural Information Processing Systems*, pages 1657–1665, 2015.
- Alessandro Rudi, Daniele Calandriello, Luigi Carratino, and Lorenzo Rosasco. On fast leverage score sampling and optimal learning. In *Advances in Neural Information Processing Systems*, pages 5672–5682, 2018.
- Fotis Savva, Christos Anagnostopoulos, and Peter Triantafillou. Explaining aggregates for exploratory analytics. In *2018 IEEE International Conference on Big Data (Big Data)*, pages 478–487. IEEE, 2018.
- John Shawe-Taylor, Nello Cristianini, et al. *Kernel methods for pattern analysis*. Cambridge university press, 2004.
- Galen R Shorack and Jon A Wellner. *Empirical processes with applications to statistics*. SIAM, 2009.
- Bernard W Silverman. Spline smoothing: the equivalent variable kernel method. *The Annals of Statistics*, pages 898–916, 1984.
- Pınar Tüfekci. Prediction of full load electrical power output of a base load operated combined cycle power plant using machine learning methods. *International Journal of Electrical Power & Energy Systems*, 60:126–140, 2014.
- Rui Tuo, Yan Wang, and CF Wu. On the improved rates of convergence for matérn-type kernel ridge regression, with application to calibration of computer models. *arXiv preprint arXiv:2001.00152*, 2020.

Aad W Van Der Vaart and Jon A Wellner. Weak convergence. In *Weak convergence and empirical processes*, pages 16–28. Springer, 1996.

Aad W van der Vaart, J Harry van Zanten, et al. Adaptive bayesian estimation using a gaussian random field with inverse gamma bandwidth. *The Annals of Statistics*, 37(5B): 2655–2675, 2009.

Linus Vepštas. An efficient algorithm for accelerating the convergence of oscillatory series, useful for computing the polylogarithm and hurwitz zeta functions. *Numerical Algorithms*, 47(3):211–252, 2008.

Grace Wahba. *Spline models for observational data*, volume 59. Siam, 1990.

G Walter, J Blum, et al. Probability density estimation using delta sequences. *the Annals of Statistics*, 7(2):328–340, 1979.

Holger Wendland. *Scattered data approximation*, volume 17. Cambridge university press, 2004.

Christopher KI Williams and Matthias Seeger. Using the nyström method to speed up kernel machines. In *Advances in neural information processing systems*, pages 682–688, 2001.

Yun Yang, Anirban Bhattacharya, and Debdeep Pati. Frequentist coverage and sup-norm convergence rate in gaussian process regression. *arXiv preprint arXiv:1708.04753*, 2017a.

Yun Yang, Mert Pilanci, Martin J Wainwright, et al. Randomized sketches for kernels: Fast and optimal nonparametric regression. *The Annals of Statistics*, 45(3):991–1023, 2017b.

The outline of the appendix is stated as follows. First, some useful results along with some proofs of the preliminaries and the main results are provided in Section A. In Section B we report the detailed settings of the experiments in the main paper. In Section C, we further analyze the properties of our leverage score approximation, which mirror the behavior of the true statistical leverage scores. To numerically accelerate the computation in the multivariate case, we simplify the multiple integral for obtaining the leverage score approximation to a single integral in Section D. Besides, we show the error caused by density estimation is negligible compared with the total error in approximating statistical leverage scores in Section E. Finally, we provide some technical facts regarding multivariate integration in Section F.

Appendix A. USEFUL FACTS

A.1. Fourier Transform

Use $L_p(\mathbb{R}^d) = \{f : \mathbb{R}^d \rightarrow \mathbb{R}, \int_{\mathbb{R}^d} |f(x)|^p dx < \infty\}$ to denote the space of all L_p integrable functions over \mathbb{R}^d for $p \geq 1$. For any function $f \in L_1(\mathbb{R}^d)$, we use $\mathcal{F}[f]$ and $\mathcal{F}^{-1}[f]$ to

denote its Fourier transform and its inverse Fourier transform, which is given by

$$\begin{aligned}\mathcal{F}[f](s) &= \int_{\mathbb{R}^d} f(x) e^{-2\pi\sqrt{-1}\langle x, s \rangle} dx, \quad \text{for all } s \in \mathbb{R}^d, \\ \mathcal{F}^{-1}[f](x) &= \int_{\mathbb{R}^d} f(s) e^{2\pi\sqrt{-1}\langle x, s \rangle} ds, \quad \text{for all } x \in \mathbb{R}^d.\end{aligned}$$

A useful property of the Fourier transform is the Parseval's identity.

Theorem 7 (Parseval's identity) *For any $f \in L_2(\mathbb{R}^d)$, the following identity holds*

$$\int_{\mathbb{R}^d} |f(x)|^2 dx = \int_{\mathbb{R}^d} |\mathcal{F}[f](s)|^2 ds.$$

Besides, Fourier transform is closely related to kernels. For any PSD stationary kernel $K : \mathbb{R}^d \times \mathbb{R}^d \rightarrow \mathbb{R}$, by Brochner's Theorem, it would be a Fourier transform of a Borel measure. For simplicity we abuse the notation by using $K(x)$ to mean $K(y, y+x)$, $\forall y \in \mathbb{R}^d$, since $K(y, y+x)$ does not depend on the specific choice of y . Specifically, the Matérn kernel K_α with smoothness parameter $\nu = \alpha - d/2 > 0$ can be equivalently defined through its Fourier transform (Rasmussen, 2003, p. 84) as

$$m_\alpha(s) := \mathcal{F}[K_\alpha](s) = \int_{\mathbb{R}^d} K_\alpha(x) e^{-2\pi\sqrt{-1}\langle x, s \rangle} dx = C_\alpha (1 + D_\alpha \|s\|^2)^{-\alpha}, \quad \forall s \in \mathbb{R}^d,$$

where C_α and D_α are some constants only dependent on α . (To simplify the statement of the theory, we would simply take $C_\alpha = D_\alpha = 1$ when later discussing the asymptotic properties.) Throughout this appendix, we focus on the case in which the Matérn kernel is used, since its theoretical properties have been well studied, and the proof is easy to be extended to other stationary kernels.

A.2. RKHS Associated with the Matérn Kernel—Proof of Theorem 1 in the Main Paper

The following theorem characterizes the RKHS \mathbb{H}_α associated with the Matérn kernel through its Fourier transform. The main body of the proof comes from the slides of Fukumizu (2008).

Lemma 8 (Fourier representation of RKHS) *For any $f, g \in \mathbb{H}_\alpha$, we have*

$$\|f\|_{\mathbb{H}_\alpha}^2 = \int_{\mathbb{R}^d} \frac{|\mathcal{F}[f](s)|^2}{m_\alpha(s)} ds, \quad \text{and} \quad \langle f, g \rangle_{\mathbb{H}_\alpha} = \int_{\mathbb{R}^d} \frac{\mathcal{F}[f](s) \cdot \overline{\mathcal{F}[g](s)}}{m_\alpha(s)} ds$$

Proof

Consider a measure space $(\mathbb{R}, \mathcal{B}, \mu)$, where $d\mu = m_\alpha(s)ds$, and $m_\alpha(s)$ is the spectral density of the invariant Matérn kernel with smoothness parameter $\nu = \alpha - \frac{d}{2}$. By referring to Section 3.1 in our main paper, we can check the function $m_\alpha(s) \in L^\infty$ is differentiable and positive everywhere. Based on the measure μ , we define a function space $\mathbb{G} = L^2(\mathbb{R}^d, \mu) \equiv \{F : \mathbb{R}^d \rightarrow \mathbb{C}; \int_{\mathbb{R}^d} |F|^2 d\mu < \infty\}$, with the inner product $\langle F, G \rangle_{\mathbb{G}} := \int F \overline{G} d\mu$. Here \mathbb{C} is the set of all complex numbers. We can observe the form is quite similar to the frequency

domain in Fourier Transform. To construct the RKHS of interest, we further define a function $H(s; x) = \exp(-2\pi\sqrt{-1}\langle x, s \rangle)$ and a map $\mathcal{M}(\cdot) : L^2(\mathbb{R}^d, \mu) \rightarrow \mathbb{T}$, similar to inverse Fourier Transform, given by

$$\mathcal{M}(F)(x) := \int F(s) \overline{H(s; x)} d\mu = \int F(s) \exp(2\pi\sqrt{-1}\langle x, s \rangle) d\mu, \quad \forall x \in \mathbb{R}^d$$

where \mathbb{T} is the space of all functions over \mathbb{R}^d with the pointwise-convergence topology, i.e. $f_n \rightarrow f \Leftrightarrow f_n(x) \rightarrow f(x), \forall x \in \mathbb{R}^d$.

Now we are able to define a new function space $\mathbb{H} := \{f \in \mathbb{T}; \exists F \in L^2(\mathbb{R}^d, \mu), f = \mathcal{M}(F)\}$, and equip it with the inner product $\langle f, g \rangle_{\mathbb{H}} := \langle F, G \rangle_{\mathbb{G}}$, where F, G satisfy $f = \mathcal{M}(F), g = \mathcal{M}(G)$. We first need to show \mathbb{H} is an RKHS. We can check for all $f \in \mathbb{H}$,

$$f(x) = \langle F, H(\cdot; x) \rangle_{\mathbb{G}} = \langle f, \mathcal{M}(H(\cdot; x)) \rangle_{\mathbb{H}}$$

Also, the reproducing kernel of \mathbb{H} would be:

$$\begin{aligned} K(x, y) &= \langle \mathcal{M}(H(\cdot; x)), \mathcal{M}(H(\cdot; y)) \rangle_{\mathbb{H}} = \langle H(\cdot; x), H(\cdot; y) \rangle_{\mathbb{G}} \\ &= \int \exp(-2\pi\sqrt{-1}\langle x, s \rangle) \exp(2\pi\sqrt{-1}\langle y, s \rangle) d\mu \\ &= \int \exp(2\pi\sqrt{-1}\langle y - x, s \rangle) m_{\alpha}(s) ds \\ &= K_{\alpha}(y - x) \end{aligned}$$

where K_{α} is the invariant Matérn kernel with smoothness parameter α . We can confirm \mathbb{H} is exactly the RKHS induced by a Matérn kernel K_{α} .

To complete the proof, we still need to find the form of $\langle f, g \rangle_{\mathbb{H}}$. Note by the facts $m_{\alpha}(s) \in L^{\infty}$ and $F \in L^2$, we can infer $F(s)m_{\alpha}(s) \in L^2$ as $\int (F(s)m_{\alpha}(s))^2 ds \leq \|m_{\alpha}\|_{\infty}^2 \int F^2(s) ds$. Using the Fourier isometry of L^2 (Adams and Fournier, 2003, Theorem 7.61), we obtain $F(s)m_{\alpha}(s) = \mathcal{F}[f](s)$; i.e., $F(s) = \mathcal{F}[f](s)/m_{\alpha}(s)$. Finally, by the definition of the inner product, for $f = \mathcal{M}(F)$ and $g = \mathcal{M}(G)$,

$$\begin{aligned} \langle f, g \rangle_{\mathbb{H}} &= \langle F, G \rangle_{\mathbb{G}} = \int \frac{\mathcal{F}[f](s)}{m_{\alpha}(s)} \overline{\frac{\mathcal{F}[g](s)}{m_{\alpha}(s)}} m_{\alpha}(s) ds \\ &= \int \frac{\mathcal{F}[f](s) \overline{\mathcal{F}[g](s)}}{m_{\alpha}(s)} ds \end{aligned}$$

in which the third equality relies on the fact the $m_{\alpha}(s)$ is real, and its conjugate is the same as itself. ■

A.3. Embedding Inequalities

Let α be an integer. Following the notation of the book (Adams and Fournier, 2003), for any $p \geq 1$ and subset $\Omega \subset \mathbb{R}^d$, we use the notation $W^{\alpha, p}(\Omega)$ to denote the Sobolev space as

a set of functions u in $L_p(\Omega)$ such that u and its weak derivatives up to total order α have a finite L_p norm. With this definition, the Sobolev space admits a norm and a seminorm

$$\|u\|_{\alpha,p,\Omega} = \left(\sum_{|\mathbf{k}| \leq \alpha} \|D^{\mathbf{k}}u\|_{p,\Omega}^p \right)^{\frac{1}{p}} = \left(\sum_{|\mathbf{k}| \leq \alpha} \int_{\Omega} |D^{\mathbf{k}}u(t)|^p dt \right)^{\frac{1}{p}}, \quad (8)$$

$$|u|_{\alpha,p,\Omega} = \left(\sum_{|\mathbf{k}|=\alpha} \int_{\Omega} |D^{\mathbf{k}}u(t)|^p dt \right)^{\frac{1}{p}}. \quad (9)$$

where $\mathbf{k} = (k_1, \dots, k_d)$ is a multi-index, and $D^{\mathbf{k}}u = \frac{\partial^{|\mathbf{k}|}u}{\partial^{k_1}x_1 \dots \partial^{k_d}x_d}$. To more precisely describe the mixed derivative, we additionally define some notations here for future use:

- \mathbf{A} is a subset of $[d]$, $-\mathbf{A} := ([d] - \mathbf{A})$,
- $u = \mathbf{I}_{\mathbf{A}} \in \{0, 1\}^d$ is a vector s.t. $u_i = 1, \forall i \in \mathbf{A}; u_i = 0, \forall i \in -\mathbf{A}$,
- a vector $u = \mu(\mathbf{A}_{-1}, \mathbf{A}_{+1}) \in \{-1, 0, 1\}^d$ satisfies $u_i = -1, \forall i \in \mathbf{A}_{-1}; u_i = 1, \forall i \in \mathbf{A}_{+1}$,
- $x_{\mathbf{A}} := (x_i)_{i \in \mathbf{A}}$, and $g(x_{\mathbf{A}}; x_{-\mathbf{A}})$ represents $g(u)$ where $u_{\mathbf{A}} = x_{\mathbf{A}}$ are the variables and $u_{-\mathbf{A}} = x_{-\mathbf{A}}$ are taken as the parameters fixed in the integration,
- $C(y, \delta) := \{(x_1, x_2, \dots, x_d); x_i \in [y_i - \delta, y_i + \delta], \forall i \in [d]\}$ is a cube centered at y ,
- $C^{\mathbf{A}}(y, \delta) = C(y_{\mathbf{A}}, \delta)$ is the marginal cube of $C(y, \delta)$ defined as $\{x_{\mathbf{A}}; x_i \in (y_i - \delta, y_i + \delta), \forall i \in \mathbf{A}\}$.

We will primarily work with the case $p = 2$ and Ω being a connected domain. For any $u \in \mathbb{H}$, by using the fact that $\mathcal{F}[D^{\mathbf{k}}u](s) = (\prod_{i=1}^d (2\pi\sqrt{-1}s_i)^{k_i}) \cdot \mathcal{F}[u](s)$ and the Parseval's identity in Theorem 7, we obtain

$$\|u\|_{\alpha,2,\mathbb{R}^d}^2 = \int_{\mathbb{R}^d} \sum_{|\mathbf{k}| \leq \alpha} \left| \prod_{i=1}^d (2\pi\sqrt{-1}s_i)^{k_i} \mathcal{F}[u](s) \right|^2 ds.$$

Since there exist constants (C_1, C_2) such that $C_1(1 + \|s\|^2)^{\alpha} \leq (\sum_{|\mathbf{k}| \leq \alpha} \prod_{i=1}^d s_i^{k_i})^2 \leq C_2(1 + \|s\|^2)^{\alpha}$ holds for all $s \in \mathbb{R}^d$, by Lemma 8 we can further deduce that

$$C_1 \|u\|_{\mathbb{H}_{\alpha}}^2 \leq \|u\|_{\alpha,2,\mathbb{R}^d}^2 \leq C_2 \|u\|_{\mathbb{H}_{\alpha}}^2 \quad (10)$$

holds for any $u \in \mathbb{H}_{\alpha}$, the RKHS associated with the Matérn kernel with smoothness index $\nu(= \alpha - d/2)$.

We first invoke the following special case of interpolation theorem of Sobolev space $W^{\alpha,p}(\Omega)$ (Adams and Fournier, 2003, Theorem 5.12).

Theorem 9 (Interpolation inequality) *For any integer $0 \leq k \leq \alpha$, there exist two constants (c_0, K) only depending on α , such that for any $u \in W^{\alpha,2}(\Omega)$ and any $\varepsilon \in (0, c_0)$,*

$$|u|_{k,2,\Omega} \leq K(\varepsilon^{\alpha-k} |u|_{\alpha,2,\Omega} + \varepsilon^{-k} \|u\|_{2,\Omega}),$$

where for any function g , $\|g\|_{2,\Omega}^2 = \int_{\Omega} g^2(t) dt$.

We will also use the following generalization of Gagliardo–Nirenberg interpolation inequalities to bound the sup-norm, which can be viewed as an extension of the above interpolation inequality to the sup-norm.

Theorem 10 (Sup-norm interpolation inequality) *There exist two universal constants (c_1, K_1) , such that for any $u \in W^{\alpha,2}(\Omega)$ and any $\varepsilon \in (0, c_1)$,*

$$\|u\|_{\infty, (1-\varepsilon^2)\Omega} := \sup_{t \in (1-\varepsilon^2)\Omega} |u(t)| \leq K_1 (\varepsilon^{-d} \|u\|_{2,\Omega} + \varepsilon^{2\alpha-d} |u|_{\alpha,2,\Omega}).$$

Proof From the Gagliardo–Nirenberg interpolation inequalities (Brezis and Mironescu, 2018), we have

$$\|g\|_{\infty,\Omega} \leq C(\|g\|_{2,\Omega} + |g|_{\alpha,\frac{d}{\alpha},\Omega}), \quad \forall g \in W^{\alpha,2}(\Omega),$$

where C is some universal constant. In fact, the last term could be further bounded by $C_0 |g|_{\alpha,2,\Omega}$ since $W^{\alpha,2} = H_\alpha$, $\alpha > \frac{d}{2}$, $\frac{d}{\alpha} < 2$, and the domain Ω is bounded.

Now for each fixed point $y_0 \in (1 - \varepsilon^2)\Omega$, we can obtain by the preceding display with $g(t) = u(y_0 + \varepsilon^2 t)$ in the above that

$$\|u\|_{\infty, B(y_0, \varepsilon^2)} \leq \varepsilon^{-d} \|u\|_{2, B(y_0, \varepsilon^2)} + C_0 \varepsilon^{2\alpha-d} |u|_{\alpha,2, B(y_0, \varepsilon^2)} \leq C \varepsilon^{-d} \|u\|_{2,\Omega} + C_0 \varepsilon^{2\alpha-d} |u|_{\alpha,2,\Omega},$$

where we have used the fact that $B(y_0, \varepsilon^2) \subset \Omega$ for any $y_0 \in (1 - \varepsilon^2)\Omega$. Finally, the claimed inequality follows by the above derivation and the fact that

$$\|u\|_{\infty, (1-\varepsilon^2)\Omega} = \sup_{y_0 \in (1-\varepsilon^2)\Omega} \|u\|_{\infty, B(y_0, \varepsilon^2)}$$

■

Theorem 9 and 10 leads to the following lemma that we will repeatedly use in our proof. Here we specifically consider a fixed point x_0 such that the density function $p(x)$ is uniformly bounded from below by $\frac{1}{2} p(x_0) > 0$ for any x satisfying $\|x - x_0\| < \delta(x_0)$ and some constant $\delta(x_0) > 0$ that may depend on x_0 . Before entering the theorem, we define an RKHS norm $\|\cdot\|_\lambda$ as

$$\|f\|_\lambda^2 = \int_{\mathbb{R}^d} f^2(x) p(x) dx + h^{2\alpha} \|f\|_{\mathbb{H}_\alpha}^2,$$

and its localized truncation $\|f\|_{x_0, \lambda}$ as

$$\|f\|_{x_0, \lambda}^2 := \int_{C(x_0, \delta(x_0))} f^2(x) p(x) dx + h^{2\alpha} \|f\|_{\mathbb{H}_\alpha}^2.$$

Theorem 11 (Local interpolation for RKHS) *Suppose $\delta(x_0) \geq Ch \log(1/h)$ for some constant $C > 0$. Let $C(x_0, \delta(x_0))$ denote a cube centered at x_0 with edge length $2\delta(x_0)$. If $C \log(1/h) > c_0^{-1}$ and $\sqrt{C \log(1/h)} > c_1^{-1}$, where (c_0, c_1) are the constants in Theorems 9 and 10, then there exists a constant K' such that*

$$|f|_{k,2,C(x_0, \delta(x_0))} \leq K' h^{-k} \max \{1, (p(x_0))^{-1/2}\} \|f\|_{x_0, \lambda},$$

for any $f \in \mathbb{H}_\alpha$ and $k = 0, 1, \dots, \alpha$. In addition, for each $k = 0, 1, \dots, \alpha$, there exists some constant $K'' > 0$ and $\varepsilon < c_1$ such that

$$\|f\|_{k, \infty, (1-\varepsilon^2)C(x_0, \delta(x_0))} \leq K'' h^{-k-d/2} \max\{1, (p(x_0))^{-1/2}\} \|f\|_{x_0, \lambda},$$

Finally, for the case $|\mathbf{A}| = k, |\mathbf{A}'| = k'$, and $\mathbf{A}' \subseteq \mathbf{A}$, there is also a constant K''' satisfying:

$$\left(\int_{C^{\mathbf{A}}(x_0, \delta(x_0))} |D^{\mathbf{1}_{\mathbf{A}'}} f(x_{\mathbf{A}}; x_{-\mathbf{A}})|^2 dx_{\mathbf{A}} \right)^{\frac{1}{2}} \leq K''' h^{-k'-(d-k)/2} \max\{1, (p(x_0))^{-1/2}\} \|f\|_{x_0, \lambda},$$

which generalizes the first inequality and provides a finer L^2 norm control.

Proof When $k = \alpha$, the first inequality is obvious due to the equivalence (10) between $\|\cdot\|_{\alpha, 2, \mathbb{R}}$ and $\|\cdot\|_{\mathbb{H}_\alpha}$, and the fact that $\|f\|_{x_0, \lambda} \geq h^\alpha \|f\|_{\mathbb{H}_\alpha}$. Now let us consider $k \leq \alpha - 1$. Let $a = \delta(x_0)$ and $u(t) = f(x_0 + at)$ for $t \in \Omega$. By applying the change of variable formula for integral and the chain rule for derivatives, we obtain (with $x = at$)

$$\begin{aligned} |u|_{k, 2, \Omega}^2 &= \sum_{|\mathbf{j}|=k} \int_{\Omega} |D^{\mathbf{j}} u(t)|^2 dt = \sum_{|\mathbf{j}|=k} a^{2k-d} \int_{C(x_0, a)} |D^{\mathbf{j}} f(x)|^2 dx \\ &= a^{2k-d} |f|_{k, 2, C(x_0, a)}^2, \quad \forall k = 0, 1, \dots, \alpha. \end{aligned}$$

Combining this with Theorem 9 and the definition (8) of Sobolev norm yields

$$\begin{aligned} |f|_{k, 2, C(x_0, \delta(x_0))}^2 &\leq a^{-(2k-d)} \left(K \varepsilon^{-k} (\varepsilon^\alpha |u|_{\alpha, 2, \Omega} + \|u\|_{2, \Omega}) \right)^2 \\ &\leq 2K^2 (a\varepsilon)^{-2k} \left((a\varepsilon)^{2\alpha} |f|_{\alpha, 2, C(x_0, \delta(x_0))}^2 + \int_{C(x_0, \delta(x_0))} |f(x)|^2 dx \right) \\ &\leq 2K^2 (a\varepsilon)^{-2k} \left((a\varepsilon)^{2\alpha} |f|_{\alpha, 2, \mathbb{R}^d}^2 + \int_{C(x_0, \delta(x_0))} |f(x)|^2 dx \right). \end{aligned}$$

Using the condition that $p(x) \geq p(x_0)/2$ for each $x \in C(x_0, \delta(x_0))$, and the equivalence (10) between $\|\cdot\|_{\alpha, 2, \mathbb{R}^d}$ and $\|\cdot\|_{\mathbb{H}_\alpha}$, we further obtain by choosing $\varepsilon = h/\delta(x_0) \leq (C \log(1/h))^{-1} < c_0$ in the above that

$$\begin{aligned} |f|_{k, 2, C(x_0, \delta(x_0))}^2 &\leq 2K^2 h^{-2k} \left(h^{2\alpha} \|f\|_{\mathbb{H}_\alpha}^2 + 2(p(x_0))^{-1} \int_{C(x_0, \delta(x_0))} |f(x)|^2 p(x) dx \right) \\ &\leq K'^2 h^{-2k} \max\{1, (p(x_0))^{-1}\} \|f\|_{x_0, \lambda}^2, \end{aligned}$$

which yields the first claimed inequality.

To prove the second inequality, we will apply Theorem 10. More specifically, we apply Theorem 10 with $u(t) = D^{\mathbf{j}} f(x_0 + at)$, $|\mathbf{j}| = k$, $a = \delta(x_0)$, $\Omega = C(x_0, \delta(x_0))$ and set $\varepsilon = \sqrt{h/a} \leq \sqrt{\frac{1}{C \log(1/h)}} < c_1$ to obtain (with a change of variable formula for integration)

$$\begin{aligned} \|D^{\mathbf{j}} f\|_{\infty, (1-\varepsilon^2)\Omega} &= \|u\|_{\infty, (1-\varepsilon^2)C(0,1)} \leq K_1 (\varepsilon^{-d} \|u\|_{2, C(0,1)} + \varepsilon^{2\alpha-2k-d} |u|_{\alpha-k, 2, C(0,1)}) \\ &\leq K_1 \varepsilon^{-d} a^{-d/2} |f|_{k, 2, \Omega} + K_1 \varepsilon^{2\alpha-2k-d} a^{\alpha-k-d/2} |f|_{\alpha, 2, \Omega} \\ &= K_1 h^{-d/2} |f|_{k, 2, \Omega} + K_1 h^{\alpha-k-d/2} |f|_{\alpha, 2, \Omega}. \end{aligned}$$

Now, we can obtain by combining the above with the first inequality of this theorem,

$$|f|_{k,\infty,(1-\varepsilon^2)\Omega} \lesssim h^{-k-d/2} \max \{1, (p(x_0))^{-1/2}\} \|f\|_{x_0,\lambda}.$$

To prove the final inequality, we will take $f(x_{\mathbf{A}}; x_{-\mathbf{A}})$ as a k -d function. Analogously using the previous result, we have:

$$\begin{aligned} \int_{C^{\mathbf{A}}} |D^{\mathbf{1}_{\mathbf{A}'}} f(x_{\mathbf{A}}; x_{-\mathbf{A}})|^2 dx_{\mathbf{A}} &\leq |f|_{k',2,C^{\mathbf{A}}}^2 \\ &\leq K'^2 h^{-2k'} \left(\int_{C^{\mathbf{A}}} f^2(x_{\mathbf{A}}; x_{-\mathbf{A}}) dx_{\mathbf{A}} + h^{2\alpha} |f(x_{\mathbf{A}}; x_{-\mathbf{A}})|_{\alpha,2,C^{\mathbf{A}}}^2 \right) \end{aligned}$$

Then we take $D^{\mathbf{g}} f(x_{\mathbf{A}}; x_{-\mathbf{A}})$ as a $(d-k)$ -d function over $C^{-\mathbf{A}}(x_0, \delta(x_0))$ (g is any multi-index whose nonzero elements are in A'), and utilize the intermediate result of the second inequality:

$$\|D^{\mathbf{g}} f(x_{\mathbf{A}}; x_{-\mathbf{A}})\|_{\infty,(1-\varepsilon^2)C^{-\mathbf{A}}} \lesssim h^{-(d-k)/2} |f|_{\mathbf{g},2,C^{-\mathbf{A}}} + h^{-(d-k)/2+(\alpha-|\mathbf{g}|)} |f|_{\alpha,2,C^{-\mathbf{A}}}.$$

In that case,

$$\begin{aligned} \int_{C^{\mathbf{A}}} f^2(x_{\mathbf{A}}; x_{-\mathbf{A}}) dx_{\mathbf{A}} &\lesssim \int_{C^{\mathbf{A}}} h^{-(d-k)} \|f(x_{\mathbf{A}}; x_{-\mathbf{A}})\|_{2,C^{-\mathbf{A}}}^2 + h^{-(d-k)+2\alpha} |f|_{\alpha,2,C^{-\mathbf{A}}}^2 dx_{\mathbf{A}} \\ &\lesssim h^{-(d-k)} \|f\|_{2,\Omega}^2 + h^{-(d-k)+2\alpha} |f|_{\alpha,2,\Omega}^2 \\ &\lesssim h^{-(d-k)} \max \{1, (p(x_0))^{-1}\} \|f\|_{x_0,\lambda}^2, \end{aligned}$$

The result for $h^{2\alpha} |f(x_{\mathbf{A}}; x_{-\mathbf{A}})|_{\alpha,2,C^{\mathbf{A}}}^2$ could be analogously obtained. Combining the pieces together, we have

$$\int_{C^{\mathbf{A}}} |D^{\mathbf{1}_{\mathbf{A}'}} f(x_{\mathbf{A}}; x_{-\mathbf{A}})|^2 dx_{\mathbf{A}} \lesssim h^{-2k'-(d-k)} \max \{1, (p(x_0))^{-1}\} \|f\|_{x_0,\lambda}^2$$

■

A.4. Leverage Score Approximation—Proof of Theorem 5 in the Main Paper

Proof Let F denote the limiting cumulative distribution function of F_n , and p the density function associated with F . Recall that the rescaled leverage approximation $\tilde{K}_{\lambda}(x, x_0)$ is the minimizer of the following local population level functional

$$A_{x_0}(f) = \frac{p(x_0)}{2} \int_{\mathbb{R}^d} f^2(x) dx + \frac{\lambda}{2} \|f\|_{\mathbb{H}_{\alpha}}^2 - f(x_0),$$

such that the following identity holds for each function $u \in \mathbb{H}_{\alpha}$, which corresponds to setting the Gateaux derivative DA_{x_0} of A_{x_0} at \tilde{K}_{x_0} to be the zero operator,

$$DA_{x_0}(\tilde{K}_{x_0})(u) = p(x_0) \int_{\mathbb{R}^d} \tilde{K}_{x_0}(x) u(x) dx + \lambda \langle \tilde{K}_{x_0}, u \rangle_{\mathbb{H}_{\alpha}} - u(x_0) = 0,$$

$$\text{or } \tilde{K}_{x_0}(x) := \tilde{K}_{\lambda}(x, x_0) = \mathcal{F}^{-1} \left[\frac{1}{p(x_0) + h^{2\alpha} (1 + \|s\|^2)^{\alpha}} \right] (x - x_0), \quad \forall x \in \mathbb{R}^d.$$

The rescaled leverage function G_{x_0} is instead the minimizer of the empirical functional A_{n,x_0} , and thus the Gateaux derivative DA_{n,x_0} at point G_{x_0} should be 0 since G_{x_0} is the optimal function for the functional. Using that fact,

$$\begin{aligned} DA_{n,x_0}(\tilde{K}_{x_0})(\tilde{u}) &= \{DA_{n,x_0}(\tilde{K}_{x_0}) - DA_{n,x_0}(G(\cdot, x_0))\}(\tilde{u}) \\ &= D^2A_{n,x_0}(G(\cdot, x_0))(\tilde{K}_{x_0} - G(\cdot, x_0), \tilde{u}) \end{aligned}$$

The last equality holds due to the definition of second order functional derivative. Note the key identity that $D^2A_{n,x_0}(G(\cdot, x_0))(\tilde{u}, \tilde{u}) = \|\tilde{u}\|_{n,\lambda}^2$. By choosing $u = \tilde{u} := \tilde{K}_{x_0} - G(\cdot, x_0)$, we would further have (u, \tilde{u}) would be used interchangeably from now on)

$$DA_{n,x_0}(\tilde{K}_{x_0})(u) = \|\tilde{u}\|_{n,\lambda}^2 = \int_{\mathbb{R}^d} \tilde{u}^2(x) dF_n(x) + \lambda \|\tilde{u}\|_{\mathbb{H}_\alpha}^2,$$

and our task somewhat reduces to bounding the term above $DA_{n,x_0}(u) = \|\tilde{K}_{x_0} - G(\cdot, x_0)\|_{n,\lambda}^2$. To do that, we can expand the expression $DA_{n,x_0}(\tilde{K}_{x_0})(u)$:

$$\begin{aligned} DA_{n,x_0}(\tilde{K}_{x_0})(u) &= \int_{\mathbb{R}^d} \tilde{K}_{x_0}(x) dF_n(x) + \lambda \langle \tilde{K}_{x_0}, u \rangle_{\mathbb{H}_\alpha} - u(x_0) \\ &= \underbrace{DA_{x_0}(\tilde{K}_{x_0})(u)}_{=0} + \underbrace{\int_{\mathbb{R}^d} \tilde{K}_{x_0}(x) u(x) d(F_n(x) - F(x))}_{=:I_1} + \underbrace{\int_{\mathbb{R}^d} \tilde{K}_{x_0}(x) u(x) (p(x) - p(x_0)) dx}_{=:I_2}, \end{aligned}$$

and bound the last two terms separately.

Using Lemma 16, as $u = \tilde{u}$ vanishes at infinity, we have

$$I_1 = (-1)^d \int_{\mathbb{R}^d} (F_n(x) - F(x)) \frac{\partial^d}{\partial x_1 \partial x_2 \cdots \partial x_d} (\tilde{K}_{x_0}(x) u(x)) dx$$

The term $|I_1|$ can be correspondingly bounded as

$$\begin{aligned} |I_1| &\leq \tau(n) \int_{\mathbb{R}^d} \left| \frac{\partial^d}{\partial x_1 \partial x_2 \cdots \partial x_d} (\tilde{K}_{x_0}(x) u(x)) \right| dx \\ &\leq \tau(n) \sum_{\mathbf{k}_1 \sqcup \mathbf{k}_2 = [d]} \int_{\mathbb{R}^d} |D^{\mathbf{k}_1} \tilde{K}_{x_0}(x) D^{\mathbf{k}_2} u(x)| dx. \end{aligned}$$

Using Lemma 12(2) about the exponential decay on \tilde{K}_{x_0} and its derivatives and the local embedding inequalities in Theorem 11, we obtain

$$\begin{aligned} \int_{\mathbb{R}^d} |D^{\mathbf{k}_1} \tilde{K}_{x_0}(x) D^{\mathbf{k}_2} u(x)| dx &\leq \int_{C_{x_0, \delta(x_0)}} |D^{\mathbf{k}_1} \tilde{K}_{x_0}(x)| |D^{\mathbf{k}_2} u(x)| dx \\ &\quad + |u|_{|\mathbf{k}_2|, 2, \mathbb{R}^d} \left(\int_{C_{x_0, \delta(x_0)}^c} |D^{\mathbf{k}_1} \tilde{K}_{x_0}(x)|^2 dx \right)^{\frac{1}{2}} \\ &\stackrel{(i)}{\leq} \left(\int_{\mathbb{R}^d} |h^{-|\mathbf{k}_1|} (h^d + h^{-d}) e^{-C_2 \|x-x_0\|/h} |^2 dx \right)^{1/2} \cdot |u|_{|\mathbf{k}_2|, 2, C_{x_0, \delta(x_0)}} \\ &\quad + |u|_{|\mathbf{k}_2|, 2, \mathbb{R}^d} \left(\int_{\|x-x_0\| \geq Ch \log(1/h)} |h^{-|\mathbf{k}_1|} (h^d + h^{-d}) e^{-C_2 \|x-x_0\|/h} |^2 dx \right)^{\frac{1}{2}} \end{aligned}$$

where step (i) follows by the Cauchy-Schwarz inequality and the assumption that $\delta(x_0) \geq Ch \log(1/h)$. Further bound is given as

$$\begin{aligned} & \int_{\mathbb{R}^d} |D^{\mathbf{k}_1} \tilde{K}_{x_0}(x) D^{\mathbf{k}_2} u(x)| dx \\ & \lesssim h^{-d/2-|\mathbf{k}_1|} |u|_{|\mathbf{k}_2|, 2, C_{x_0, \delta(x_0)}} + \log^{\frac{d-1}{2}}(1/h) h^{C_2 C - d/2 - |\mathbf{k}_1|} |u|_{|\mathbf{k}_2|, 2, \mathbb{R}^d} \\ & \stackrel{(ii)}{\lesssim} h^{-d/2-|\mathbf{k}_1|-|\mathbf{k}_2|} \max \{1, (p(x_0))^{-1/2}\} \|u\|_{x_0, \lambda} + \log^{\frac{d-1}{2}}(1/h) h^{C_2 C - d/2 - |\mathbf{k}_1|} |u|_{|\mathbf{k}_2|, 2, \mathbb{R}^d}, \end{aligned}$$

where step (ii) uses the first inequality in Theorem 11 with $k = |\mathbf{k}_2|$. The next bound is derived as,

$$\begin{aligned} & \int_{\mathbb{R}^d} |D^{\mathbf{k}_1} \tilde{K}_{x_0}(x) D^{\mathbf{k}_2} u(x)| dx \\ & \lesssim h^{-3d/2} \max \{1, (p(x_0))^{-1/2}\} \|u\|_{x_0, \lambda} + \log^{\frac{d-1}{2}}(1/h) h^{C_2 C - d/2 - |\mathbf{k}_1|} |u|_{|\mathbf{k}_2|, 2, \mathbb{R}^d} \\ & \lesssim h^{-3d/2} \max \{1, (p(x_0))^{-1/2}\} \|u\|_{x_0, \lambda} + \log^{\frac{d-1}{2}}(1/h) h^{C_2 C - d/2 - |\mathbf{k}_1| - \alpha} \|u\|_{x_0, \lambda}, \end{aligned}$$

in which the last step utilizes the fact that $\|u\|_{1, 2, \mathbb{R}} \leq \|u\|_{\mathbb{H}_\alpha} \leq h^{-\alpha} \|u\|_{x_0, \lambda}$. For $C > \alpha/C_2$, we can finally obtain

$$|I_1| \lesssim \tau(n) h^{-3d/2} \max \{1, (p(x_0))^{-1/2}\} \|u\|_{x_0, \lambda}.$$

Similarly, by using the Lipschitz property of the density function p as $|p(x) - p(x_0)| \leq \min \{2C_p, L_{x_0} \|x - x_0\|\}$ (where $C_p = \sup_x |p(x)|$ and L_{x_0} is the local Lipschitz constant of p around x_0), the exponential decay on \tilde{K}_{x_0} and the local embedding inequalities in Theorem 11 with $k = 0$, we obtain

$$\begin{aligned} |I_2| & \lesssim \int_{C_{x_0, \delta(x_0)}} |\tilde{K}_{x_0}(x)| \cdot \|x - x_0\| \cdot |u(x)| dx + \|u\|_{\infty, \mathbb{R}^d} \int_{C_{x_0, \delta(x_0)}^c} |\tilde{K}_{x_0}(x)| dx \\ & \lesssim \left(\int_{\mathbb{R}^d} |(h^d + h^{-d}) e^{-C_2 \|x - x_0\|/h} \|x - x_0\|^2 dx \right)^{1/2} \cdot \|u\|_{2, C_{x_0, \delta(x_0)}} \\ & \quad + \|u\|_{\infty, \mathbb{R}^d} \int_{\|x - x_0\| \geq Ch \log(1/h)} |(h^d + h^{-d}) e^{-C_2 \|x - x_0\|/h}| dx \\ & \lesssim h^{-d/2+1} \|u\|_{2, C_{x_0, \delta(x_0)}} + h^{C_2 C} \|u\|_{\infty, \mathbb{R}^d} \\ & \lesssim h^{-d/2+1} \max \{1, (p(x_0))^{-1/2}\} \|u\|_{x_0, \lambda} + h^{C_2 C} \|u\|_{\infty, \mathbb{R}^d}. \end{aligned}$$

Putting pieces together, we obtain

$$|DA_{n, x_0}(\tilde{K}_{x_0})(u)| \lesssim h^{C_2 C} \|u\|_{\infty} + \max \{1, (p(x_0))^{-1/2}\} (\tau(n) h^{-3d/2} + h^{-d/2+1}) \|u\|_{x_0, \lambda}.$$

Now we return back to the right hand side of the identity $DA_{n, x_0}(\tilde{K}_{x_0})(u) = \|\tilde{u}\|_{n, \lambda}^2$. Since F_n is nondecreasing, we have the following bound,

$$\begin{aligned} \int_{\mathbb{R}^d} \tilde{u}^2(x) dF_n(x) & \geq \int_{C(x_0, \delta(x_0))} \tilde{u}^2(x) dF_n(x) \\ & = \int_{C(x_0, \delta(x_0))} \tilde{u}^2(x) dF(x) + \int_{C(x_0, \delta(x_0))} \tilde{u}^2(x) d(F_n(x) - F(x)). \end{aligned}$$

Therefore, by the definition of the localized norm $\|\cdot\|_{x_0, \lambda}$, we have

$$\|\tilde{u}\|_{n, \lambda}^2 \geq \|\tilde{u}\|_{x_0, \lambda}^2 + \underbrace{\int_{C(x_0, \delta(x_0))} \tilde{u}^2(x) d(F_n(x) - F(x))}_{=: I_3}.$$

By applying the Lemma 16 again (note \tilde{u} and \tilde{u}^2 are infinitely differentiable), the second term I_3 can be bounded as (some terms are hidden)

$$\begin{aligned} |I_3| &\lesssim \|\tilde{u}^2(x) (F_n(x) - F(x))\|_{\infty, C_{x_0, \delta(x_0)}} + \dots \\ &\quad + \|F_n(x) - F(x)\|_{\infty, C_{x_0, \delta(x_0)}} \int_{C_{x_0, \delta(x_0)}} \left| \frac{\partial^d}{\partial x_1 \partial x_2 \dots \partial x_d} (\tilde{u}^2(x)) \right| dx. \end{aligned}$$

Now by applying the first and the second inequality in Theorem 11, and the Cauchy-Schwarz inequality, the sum of the two terms above can be bounded up to a constant by

$$\max \{1, (p(x_0))^{-1}\} \tau(n) h^{-d} \|\tilde{u}\|_{x_0, \lambda}^2.$$

Putting all the pieces together, we can reach

$$\begin{aligned} &(1 - c\tau(n) \max \{1, (p(x_0))^{-1}\} h^{-d}) \|\tilde{u}\|_{x_0, \lambda}^2 \\ &\leq c' h^{C_2 C} \|\tilde{u}\|_{\infty} + c' \max \{1, (p(x_0))^{-1/2}\} (\tau(n) h^{-3d/2} + h^{-d/2+1}) \|\tilde{u}\|_{x_0, \lambda}. \end{aligned}$$

It is easy to verify directly that we always have the crude bound $\|\tilde{u}\|_{\infty} \lesssim n$, so by choosing constant C sufficiently large $h^{C_2 C} n$ is decreasing, we can obtain from the above that

$$\|\tilde{u}\|_{x_0, \lambda} \lesssim \max \{1, (p(x_0))^{-1/2}\} (\tau(n) h^{-3d/2} + h^{-d/2+1}).$$

In addition, an application of the second inequality in Theorem 11 implies

$$\sup_{x \in C_{x_0, (1-h)\delta(x_0)}} |\tilde{u}(x)| \lesssim \max \{1, (p(x_0))^{-1/2}\} (\tau(n) h^{-2d} + h^{-d+1}).$$

Finally, by taking $x = y = x_0$ in the integral form of \tilde{K}_{x_0} in equation (11), we have the lower bound $\tilde{K}_{x_0}(x_0) \geq c h^{-d} (p(x_0))^{-1+1/(2\alpha)}$ for some constant $c > 0$ that only depends on α . Therefore, we have the relative error bound

$$\frac{|\tilde{K}_{\lambda}(x_0, x_0) - G(x_0, x_0)|}{|G(x_0, x_0)|} \lesssim \max \{1, (p(x_0))^{1/2-1/(2\alpha)}\} \sqrt{p(x_0)} (\tau(n) h^{-d} + h),$$

for any x_0 such that the density function satisfies $p(x) \geq p(x_0)/2$ for all x in an $h \log(1/h)$ neighborhood of x_0 . In particular, for any $\alpha \geq 1$, the relative error of estimating the leverage score remains bounded even if the local density $p(x_0)$ tends to zero. \blacksquare

Appendix B. MORE ON SIMULATIONS

In this section, we mainly provide the complete experiment settings and one additional figure to help illustrate our method. We first describe all the competing methods: original kernel ridge regression; Nyström methods with uniform sampling (hereinafter referred to as "vanilla"); Nyström with Recursive-RLS (RC) (Musco and Musco, 2017); Nyström with BLESS (Rudi et al., 2018); and Nyström with spectral analysis (SA, our proposed method).

B.1. Experiment Settings in Figure 1 in the Main Paper

In this experiment, we compare the runtime and runtime versus error trade-off among Vanilla, RC, BLESS, and our method SA in Figure 1, under the 3-d bimodal setting ($\gamma = 0.4$) using the Matérn kernel ($\nu = 1.5$). Specifically, the bimodal distribution has two components: with probability $\frac{n}{n+n^\gamma}$ generating a $\text{Unif}[0, 1]^3$; and with probability $\frac{n^\gamma}{n+n^\gamma}$ generating a random variable with pdf $\prod_{j=1}^3 (5 - 2x_j)$ for $x_j \in [2, 2.5]$, where n is the sample size.

The sample size n ranges from 2,000 to 500,000. In particular, the target function is set as $f^*(x) = g(\|x\|_2/d)$ with $g(x) = 1.6|(x - 0.4)(x - 0.6)| - x(x - 1)(x - 2) - 0.5$, and i.i.d. noises follow $\mathcal{N}(0, 0.25)$; regularization parameter λ is set as $0.075 \cdot n^{-2/3}$, and the bandwidth for Gaussian kernel density estimator is $0.15n^{-1/7}$. The KDE estimator allows a 0.15 relative error. The projection dimension for all the methods is set as $5 \cdot n^{1/3}$, while the sub-sampling size s for all the iteration-based Nyström methods listed is chosen as $1 \cdot n^{1/3}$ due to high time complexity. All the results reported in Figure 1 are averaged over 30 replicates.

B.2. Experiment Settings in Table 1 in the Main Paper

Each method above is run on the RadiusQueriesCount (Savva et al., 2018; Anagnostopoulos et al., 2018) (denoted by RQP), HTRU2 (Lyon et al., 2016), and CCPP (Tüfekci, 2014; Kaya and Tüfekci, 2012) datasets downloaded from the UCI ML Repository (Dua and Graff, 2017). Those datasets contain 10000, 17898, and 9568 data points, with 3, 8, and 5 features respectively. The smoothness parameter of Matérn kernel is set as $\nu = 0.5$, and $\alpha := \nu + \frac{d}{2} = \frac{d}{2} + 0.5$. The regularization parameter λ is set as $0.15 \cdot n^{-\frac{2\alpha}{2\alpha+d}}$. To attain the optimal error rate, the projection dimension of all methods $\lfloor 2 \cdot n^{\frac{d}{2\alpha+d}} \rfloor$; while the sub-sample size for estimating the statistical leverage scores in RC and BLESS is set as $\lfloor 1 \cdot n^{\frac{d}{2\alpha+d}} \rfloor$. We still use kernel density estimator to gain density estimation, and the detailed setting of this estimator is almost the same as the last experiment, using Gaussian kernel and the bandwidth $0.5 \cdot n^{-\frac{1}{3}}$. All the results reported in Table 1 are averaged over 10 replicates.

B.3. Experiment Settings in Figure 2 in the Main Paper

We ran the experiments on the one-dimensional (for the ease of visualization) $\text{Unif}[0, 1]$, $\text{Beta}(15, 2)$, and a bimodal distribution, as before, with two components: with probability $\frac{n}{n+n^\gamma}$ generating a $\text{Unif}[0, 0.5]$; and with probability $\frac{n^\gamma}{n+n^\gamma}$ generating a random variable with pdf $(3 - 2x)$ for $x \in [1, 1.5]$, where n is the sample size and $\gamma = 0.6$. In addition, the Matérn kernel with smoothness parameter $\nu = 1.5$ is used, and density estimation is performed by

a tree-based kernel density estimator. The number of observations varies from $n = 200$ to $10,000$. The regularization parameter of the KRR is set as $\lambda = 0.45 \cdot n^{-0.8}$.

A Gaussian kernel is used for density estimation, and the bandwidth is set to $1 \cdot n^{-0.2}$ for Uniform $[0, 1]$ and $0.3 \cdot n^{-1/3}$ for the rest two distributions. Also, we allow a 0.05 relative error tolerance for density estimation since highly accurate density estimation is not required for Nyström methods (cf. Section E). While implementing our algorithm, we also apply an ad-hoc modification to avoid the potential instability with a small density value $p(x_i)$, as mentioned in Section 3.1 in the main paper. Particularly, in the case of Beta distribution, if the density of point x_i is smaller than a threshold $h = 0.3 \cdot n^{-0.8}$, a weighted average $\frac{0.5h+p(x_i)}{1.5}$ would be used for the subsequent leverage score approximation.

In Figure 2, we show our method provides reasonably good approximations to the rescaled leverage scores across all settings. In particular, Unif $[0, 1]$ is the easiest case (red curves) due to its flat density, which meets Assumption 3 and 4 for almost all design points; while for points with low density, such as those in the smaller cluster of the bimodal distribution and close to the boundary of Beta(15, 2), the absolute error tends to be large due to the leading constant C_{x_0} in the error bound in Theorem 5. Moreover, the relative approximation error has a clear tendency of decreasing as the sample size increases, which is also consistent with our theory.

B.4. The Additional Experiment for Gaussian Kernels

To show that our proposed method can also be extended to more kernels other than Matérn kernels, in this subsection we compare the in-sample prediction error among the methods above in Figure 3, under a dimension-increasing setting ($d = 3, 10, 30$ respectively) using a Gaussian kernel with bandwidth $\sigma = 1.5n^{-\frac{1}{2d+3}}$. We still use a bimodal distribution similar to the above one: ($\gamma = 0.4$) with probability $\frac{n}{n+n^\gamma}$ generating a Unif $[0, 1]^d$; and with probability $\frac{n^\gamma}{n+n^\gamma}$ generating a random variable with pdf $\prod_{j=1}^d (7 - 2x_j)$ for $x_j \in [3, 3.5]$, where n is the sample size.

The sample size n ranges from 1000 to 100,000. In particular, the target function is set as $f^*(x) = g(\|x\|_2/d) + g(x_1)$ (x_1 is the first element of x) with $g(x) = 1.6|(x - 0.4)(x - 0.6)| - x(x - 1)(x - 2) - 0.5$, and i.i.d. noises follow $\mathcal{N}(0, 0.25)$, which is the same as before; regularization parameter λ is set as $0.075 \cdot n^{-\frac{d+3}{2d+3}}$, and the bandwidth for the used Gaussian kernel density estimator is tuned for different dimension since when d is large, the density estimation will greatly fluctuate with the size of bandwidth. The projection dimension for all the methods is set as $5 \cdot n^{\frac{d}{2d+3}}$, while the sub-sampling size s for all the iteration-based Nyström methods listed is chosen as $1 \cdot n^{\frac{d}{2d+3}}$ due to high time complexity. All the results reported in Figure 1 are averaged over 20 replicates. From Figure 3, we observe when d increases, all the leverage-based methods will be no longer significantly better than vanilla uniform sampling, and the in-sample prediction error becomes orders of magnitude larger. We remark here that an increasing d indeed theoretically violates the assumption of kernel methods on the dimension. For the bad performance of KRR, we conjecture that is because in a high dimensional space the input samples get sparser (regarding the Euclidean distance), and thus roughly speaking for a certain sample with high density it is also hard to find some points around the sample, which is similar to the case for samples with low density.

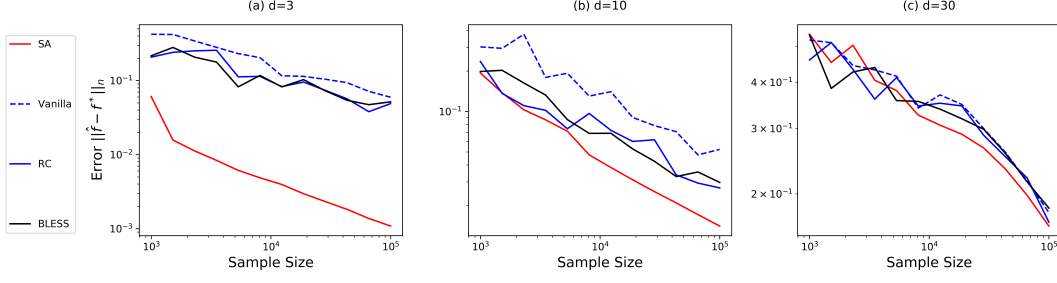


Figure 3: In-sample prediction error for Gaussian kernels with increasing dimension.

Appendix C. APPROXIMATION PROPERTIES

In this section, we prove some useful properties of our equivalent kernel approximation introduced by Matérn kernels. Some parts of the proof rely on the isotropy of the stationary kernels. Since the isotropy is a property shared by most common stationary kernels, the proof is expected to be applied to other stationary kernels as well. For the reader's convenience, we also prove the corresponding lemmas for Gaussian kernels in Appendix C.2. The proof strategy across the section is as follows, we first focus on one-dimensional cases and utilize the results to prove the conclusion for general multivariate approximation.

C.1. Matérn Kernel

For simplicity, we ignore some constants (such as $p(x_0)$ that does not change the local shape and scale of $\tilde{K}_\lambda(\cdot, x_0)$) and instead consider the rescaled leverage approximation specified by

$$\tilde{K}_\lambda(x, y) = \tilde{K}_\lambda(x - y) = \int_{\mathbb{R}^d} \frac{e^{2\pi\sqrt{-1}\langle s, x-y \rangle}}{1 + \lambda(1 + \|s\|^2)^\alpha} ds = \int_{\mathbb{R}^d} \frac{\cos(2\pi\langle s, x - y \rangle)}{1 + \lambda(1 + \|s\|^2)^\alpha} ds, \quad (11)$$

where $\lambda = h^{2\alpha}$. By the inverse Fourier transform, we have

$$f_\lambda(s) = \frac{1}{1 + \lambda(1 + \|s\|^2)^\alpha} = \int_{\mathbb{R}^d} \tilde{K}_\lambda(u) e^{-2\pi\sqrt{-1}\langle s, u \rangle} du. \quad (12)$$

Lemma 12 *When $2\alpha = 2\nu + d \geq d + 1$ is an integer, we have:*

1. $\|\tilde{K}_\lambda\|_\infty \lesssim h^{-d}$;
2. *There exists some constants $C_2 > 0$ such that*

$$|D^{\mathbf{j}} \tilde{K}_\lambda(x, y)| \leq (h^{-|\mathbf{j}|-d}) e^{-C_2 \|x-y\|/h}, \quad |\mathbf{j}| = 0, 1, \dots, d.$$

Proof

We start with the proof for the univariate case. From equation (11), we have

$$\|\tilde{K}_\lambda\|_\infty \leq \int_{-\infty}^{\infty} \frac{1}{1 + \lambda(1 + s^2)^\alpha} ds \leq \int_{-\infty}^{\infty} \frac{1}{1 + \lambda s^{2\alpha}} ds \lesssim \lambda^{-1/(2\alpha)} = h^{-1},$$

which is the first claimed property.

To prove the second property, we will apply the residue theorem to the following function

$$g(z) = \frac{e^{2\pi\sqrt{-1}|u|z}}{1 + h^{2\alpha}(1 + z^2)^\alpha}, \quad z \in \mathbb{C},$$

which is holomorphic on $\mathbb{C} \setminus \{z_1, \dots, z_{2\alpha}\}$, where $z_1, \dots, z_{2\alpha}$ are the 2α roots to the equation

$$1 + h^{2\alpha}(1 + z^2)^\alpha = 0.$$

Therefore, z_{2k-1} and z_{2k} , for $k = 1, \dots, \alpha$, are the two roots of the equation

$$z^2 = h^{-2} e^{\sqrt{-1} \frac{2k-1}{\alpha} \pi} - 1,$$

and $z_{2k-1} = -z_{2k}$. Without loss of generality, we assume $\text{Im}(z_{2k-1}) > 0$. Direct calculations show that $|\text{Im}(z_{2k-1})| \gtrsim h^{-1}$ and $|z_{2k-1}| \lesssim h^{-1}$ for each $k = 1, \dots, \alpha$. Now we apply the residue theorem to the following contour integral

$$\int_C g(z) dz = \int_C \frac{e^{2\pi\sqrt{-1}|u|z}}{1 + h^{2\alpha}(1 + z^2)^\alpha} dz,$$

where the contour C goes along the real line from $-R$ to R and then counter-clockwise along a semicircle centering at 0 from R to $-R$, for some sufficiently large constant $R > 0$. The residue theorem implies

$$\int_C g(z) dz = 2\pi\sqrt{-1} \sum_{k=1}^{\alpha} \frac{e^{2\pi\sqrt{-1}|u|z_{2k-1}}}{2\alpha h^{2\alpha}(1 + z_{2k-1}^2)^{\alpha-1} z_{2k-1}},$$

where we have used the fact that $\{z_{2k-1}\}_{k=1}^{\alpha}$ are the singularity points inside the contour C . Since $1 + h^{2\alpha}(1 + z_{2k-1}^2)^\alpha = 0$, the above can be further simplified into

$$\int_C g(z) dz = -\pi\sqrt{-1} \sum_{k=1}^{\alpha} \frac{e^{2\pi\sqrt{-1}|u|z_{2k-1}}(1 + z_{2k-1}^2)}{\alpha z_{2k-1}}.$$

Due to the aforementioned properties that $|\text{Im}(z_{2k-1})| \gtrsim h^{-1}$ and $|z_{2k-1}| \lesssim h^{-1}$, we have

$$\left| \int_C g(z) dz \right| \lesssim (h + h^{-1}) e^{-C|u|/h}.$$

Finally, we can split the contour C into a straight part (real line) and a curved arc, so that

$$\int_C g(z) dz = \int_{(-R, R)} g(z) dz + \int_{\text{arc}} g(z) dz,$$

where the arc part satisfies

$$\left| \int_{\text{arc}} g(z) dz \right| \leq \pi R \cdot \sup_{\text{arc}} \left| \frac{e^{2\pi\sqrt{-1}|u|z}}{1 + h^{2\alpha}(1 + z^2)^\alpha} \right| \leq \frac{\pi R}{h^{2\alpha}(R^2 - 1)^\alpha - 1}.$$

By taking $R \rightarrow \infty$ (note that $\alpha > 1/2$) and putting all pieces together, we finally reach

$$|\tilde{K}_\lambda(x - y)| = \left| \int_{-\infty}^{\infty} \frac{e^{2\pi\sqrt{-1}s(x-y)}}{1 + \lambda(1 + s^2)^\alpha} ds \right| \lesssim (h + h^{-1}) e^{-C|x-y|/h},$$

which is part of the second desired property.

To complete the proof of the second property, we still need to bound the derivative of the equivalent kernel. Recall the differentiation property of Fourier transform, and $\mathcal{F}[\tilde{K}'_\lambda]$ could be written as:

$$\mathcal{F}[\tilde{K}'_\lambda] = \frac{2\pi\sqrt{-1}s}{1 + h^{2\alpha}(1 + s^2)^\alpha}$$

Following a similar way, we can accordingly reset function g as:

$$g(z) = \frac{e^{2\pi\sqrt{-1}|u|z} 2\pi\sqrt{-1}z}{1 + h^{2\alpha}(1 + z^2)^\alpha}, \quad z \in \mathbb{C},$$

and by the same procedure obtain the following equality

$$\int_C g(z) dz = 4\pi^2 \sum_{k=1}^{\alpha} \frac{e^{2\pi\sqrt{-1}|u|z_{2k-1}} (1 + z_{2k-1}^2)^{2k-1}}{2\alpha z_{2k-1}} = 2\frac{\pi^2}{\alpha} \sum_{k=1}^{\alpha} e^{2\pi\sqrt{-1}|u|z_{2k-1}} (1 + z_{2k-1}^2).$$

As for the integral over the arc part, its value is still negligible due to a finer control. Note over the arc, $z = R\cos(\theta) + \sqrt{-1}R\sin(\theta)$, $\theta \in [0, \pi]$, and

$$\begin{aligned} & \left| \int_{\text{arc}} g(z) dz \right| \\ &= \left| 2\pi\sqrt{-1} \int_0^\pi e^{-2\pi|u|R\sin(\theta)} \frac{e^{2\pi\sqrt{-1}|u|R\cos(\theta)} z(\theta)}{1 + h^{2\alpha}(1 + z^2(\theta))^\alpha} (-R\sin(\theta) + \sqrt{-1}R\cos(\theta)) d\theta \right| \\ &\leq \frac{2\pi^2 R^2}{h^{2\alpha}(R^2 - 1)^\alpha - 1} \cdot 2 \int_0^{\frac{\pi}{2}} e^{-2\pi|u|R\sin(\theta)} d\theta. \end{aligned}$$

To bound the rest integral, we utilize the fact that $\sin(\theta)/\theta$ is decreasing in $(0, \pi/2]$, and $\sin(\theta) \geq \frac{2}{\pi}\theta$, $\forall \theta \in (0, \pi/2]$. Therefore,

$$\left| \int_{\text{arc}} g(z) dz \right| \leq \frac{2\pi^2 R^2}{h^{2\alpha}(R^2 - 1)^\alpha - 1} \cdot 2 \int_0^{\frac{\pi}{2}} e^{-4|u|R\theta} d\theta \leq \frac{C}{|u|} \frac{\pi^2 R}{h^{2\alpha}(R^2 - 1)^\alpha - 1}.$$

By taking $R \rightarrow \infty$ (note that $2\alpha > d = 1$ here), the magnitude of the integral over the arc would vanish.

Putting all pieces together, we finally reach

$$|\tilde{K}'_\lambda(x - y)| = \left| \int_{-\infty}^{\infty} \frac{e^{2\pi\sqrt{-1}s(x-y)} (2\pi\sqrt{-1}s)}{1 + \lambda(1 + s^2)^\alpha} ds \right| \lesssim (1 + h^{-2}) e^{-C|x-y|/h},$$

which complete the proof of the second property for univariate cases.

The proof for the multivariate claim will utilize the univariate conclusion before. By using the polar coordinate transform in Appendix D, we can reduce the original multivariate integral to a univariate one (cf. equation (14)). The rescaled leverage $\tilde{K}_\lambda(0)$ would be proportional to:

$$\int_0^\infty \frac{r^{d-1}}{1 + \lambda(1 + r^2)^\alpha} dr.$$

which is of the scale h^{-d} by using the same technique as before. Therefore the first claim in this lemma has been proved.

For the second claim, we would heavily utilize the isotropy trick to simplify the proof. By the isotropy of Matérn kernels and our $\tilde{K}_\lambda(u)$, we only need to consider a special input $\tilde{u} = (\|u\|, 0, \dots, 0)$. That is motivated by the observation that we can always do the coordinate transformation $s = T \cdot t$, where T is an orthogonal matrix and its first row $T_{1,\cdot} = u/\|u\|$. In that case, the original mixed derivative $D^{\mathbf{j}} \tilde{K}_\lambda(u)$ could be expressed as

$$\int_{\mathbb{R}^d} \frac{e^{2\pi\sqrt{-1}\langle u, s \rangle}}{1 + h^{2\alpha}(1 + \|s\|^2)^\alpha} \prod_{i=1}^d (2\pi\sqrt{-1}s_i)^{\mathbf{j}_i} ds = \int_{\mathbb{R}^d} \frac{e^{2\pi\sqrt{-1}\|u\|t_1}}{1 + h^{2\alpha}(1 + \|t\|^2)^\alpha} \prod_{i=1}^d (2\pi\sqrt{-1}\langle T_{i,\cdot}, t \rangle)^{\mathbf{j}_i} dt,$$

which is of the same scale as $\max_{|\mathbf{j}'|=|\mathbf{j}|} |D^{\mathbf{j}'} \tilde{K}_\lambda(\tilde{u})|$. Under the settings above, the target considered would be reduced to

$$\begin{aligned} & \left| \int_{\mathbb{R}^d} \frac{e^{2\pi\sqrt{-1}\|u\|s_1}}{1 + h^{2\alpha}(1 + \sum_{i=1}^{d-1} s_i^2 + s_d^2)^\alpha} \prod_{i=1}^d (s_i)^{\mathbf{j}_i} ds \right| \\ &= \left| \int_{\mathbb{R}^{d-1}} \prod_{i=2}^d (s_i)^{\mathbf{j}_i} \int_{-\infty}^\infty \frac{e^{2\pi\sqrt{-1}\|u\|s_1} s_1^{\mathbf{j}_1}}{1 + h^{2\alpha}(1 + \|s_{-1}\|^2 + s_1^2)^\alpha} ds_1 ds_{-1} \right| \\ &\leq \int_{\mathbb{R}^{d-1}} \prod_{i=2}^d |s_i|^{\mathbf{j}_i} \left| \int_{-\infty}^\infty \frac{e^{2\pi\sqrt{-1}\|u\|s_1} s_1^{\mathbf{j}_1}}{1 + h^{2\alpha}(1 + \|s_{-1}\|^2 + s_1^2)^\alpha} ds_1 \right| ds_{-1}. \end{aligned}$$

The next important step is to take the expression $1 + \|s_{-1}\|^2$ as a constant, and again apply the residue theorem to bound the internal integral as

$$\begin{aligned} & \left| \frac{\pi\sqrt{-1}}{\alpha} \sum_{k=1}^\alpha e^{2\pi\sqrt{-1}\|u\|z_{2k-1}} (1 + z_{2k-1}^2) (z_{2k-1})^{\mathbf{j}_1-1} \right| \\ &= \left| \frac{\pi}{\alpha} \sum_{k=1}^\alpha e^{2\pi\sqrt{-1}\|u\|z_{2k-1}} h^{-2} e^{\sqrt{-1}\frac{2k-1}{\alpha}\pi} (z_{2k-1})^{\mathbf{j}_1-1} \right|, \end{aligned}$$

where $z_{2k-1} := a_k + \sqrt{-1} \cdot b_k$, and if we denote $\theta_k := \frac{2k-1}{\alpha}\pi$,

$$\begin{aligned} a_k^2 + b_k^2 &= |z_{2k-1}|^2 = (h^{-4} \sin^2(\theta_k) + (h^{-2} \cos(\theta_k) - \|s_{-1}\|^2 - 1)^2)^{\frac{1}{2}}, \\ 2b_k^2 &= (a_k^2 + b_k^2) - (a_k^2 - b_k^2) \\ &= (h^{-4} \sin^2(\theta_k) + (h^{-2} \cos(\theta_k) - \|s_{-1}\|^2 - 1)^2)^{\frac{1}{2}} - (h^{-2} \cos(\theta_k) - \|s_{-1}\|^2 - 1) \\ &= \frac{h^{-4} \sin^2(\theta_k)}{(h^{-4} \sin^2(\theta_k) + (h^{-2} \cos(\theta_k) - \|s_{-1}\|^2 - 1)^2)^{\frac{1}{2}} + (h^{-2} \cos(\theta_k) - \|s_{-1}\|^2 - 1)} \end{aligned}$$

Note this time the magnitude of $\|s_{-1}\|$ matters a lot, and we need to divide the outside integral into two domains, $D_1 := \{|h^{-2} \cos(\theta_k) - \|s_{-1}\|^2 - 1| \leq 3h^{-2} |\cos(\theta_k)|\}$ and $D_2 := \{|h^{-2} \cos(\theta_k) - \|s_{-1}\|^2 - 1| > 3h^{-2} |\cos(\theta_k)|\}$.

Over domain D_1 , we can imply $\|s_{-1}\|^2 \leq 4h^{-2}$, and similar to the univariate case we can have $b_k \gtrsim h^{-1}$ and $|z_{2k-1}| = \sqrt{a_k^2 + b_k^2} = \Theta(h^{-1})$. The corresponding integral would be bounded by a constant multiple of

$$\begin{aligned} & \int_{D_1} \prod_{i=2}^d |s_i|^{\mathbf{j}_i} h^{-2} e^{-C\|u\|b_k} (z_{2k-1})^{\mathbf{j}_1-1} ds_{-1} \\ & \lesssim \int_{\|s_{-1}\|^2 \leq 4h^{-2}} \|s_{-1}\|^{\|\mathbf{j}\|-\mathbf{j}_1} h^{-2} e^{-C\|u\|h^{-1}} h^{-(\mathbf{j}_1-1)} ds_{-1} \\ & \lesssim e^{-C\|u\|h^{-1}} h^{-(\mathbf{j}_1+1)} \int_0^{2h^{-1}} r^{\|\mathbf{j}\|-\mathbf{j}_1+d-2} dr \lesssim e^{-C\|u\|h^{-1}} h^{-\|\mathbf{j}\|-d}. \end{aligned}$$

For domain D_2 , we could notice b_k would be much bigger than in D_1 as now $\|s_{-1}\|$ tends to dominate h^{-1} . Specifically, $2b_k^2 \geq 1 + \|s_{-1}\|^2 + h^{-2}(1 - \cos(\theta_k))$ and thus $b_k \geq C(\|s_{-1}\| + h^{-1})$. Considering $|z_{2k-1}| = \Theta(\|s_{-1}\|)$, we have

$$\begin{aligned} & \int_{D_2} \prod_{i=2}^d |s_i|^{\mathbf{j}_i} h^{-2} e^{-C\|u\|b_k} (z_{2k-1})^{\mathbf{j}_1-1} ds_{-1} \\ & \lesssim h^{-2} e^{-C\|u\|h^{-1}} \int_{\|s_{-1}\|^2 > c^2 h^{-2}} \|s_{-1}\|^{\|\mathbf{j}\|-\mathbf{j}_1} e^{-C\|u\|\|s_{-1}\|} \|s_{-1}\|^{\mathbf{j}_1-1} ds_{-1} \\ & \lesssim h^{-2} e^{-C\|u\|h^{-1}} \int_{ch^{-1}}^{\infty} r^{\|\mathbf{j}\|+d-3} e^{-C'\|u\|r} dr \lesssim h^{-2} e^{-C\|u\|h^{-1}} h^{-\|\mathbf{j}\|-d+3} e^{-C'\|u\|h^{-1}} \\ & \lesssim e^{-C\|u\|h^{-1}} h^{-\|\mathbf{j}\|-d+1} \lesssim e^{-C\|u\|h^{-1}} h^{-\|\mathbf{j}\|-d}. \end{aligned}$$

Combining the two pieces, we finally have

$$|D^{\mathbf{j}} \tilde{K}_\lambda(u)| \lesssim e^{-C\|u\|h^{-1}} h^{-\|\mathbf{j}\|-d}.$$

■

C.2. Gaussian Kernel

Similarly, we specify the equivalent kernel as

$$\tilde{K}_\lambda(x, y) = \int_{\mathbb{R}^d} \frac{e^{2\pi\sqrt{-1}\langle s, x-y \rangle}}{1 + \frac{\lambda}{\sigma^d} e^{\|\sigma s\|^2}} ds = \int_{\mathbb{R}^d} \frac{\cos(2\pi \langle s, x-y \rangle)}{1 + \frac{\lambda}{\sigma^d} e^{\|\sigma s\|^2}} ds, \quad (13)$$

where the bandwidth σ is introduced due to its importance to exponential kernels. The scale of the bandwidth is set as $\mathcal{O}(\lambda^{\frac{1}{2\alpha}})$, where α is the corresponding parameter of the most suitable Matérn kernel attaining the optimal error rate in kernel ridge regression problems. We also define an auxiliary parameter h as $h^{-2} \equiv \ln \frac{\sigma^d}{\lambda}$ for simplicity of notation. In practice, σ would be specified in a way similar to Matérn case; a parameter $\alpha > d/2$ would be first chosen, and then let $\sigma = \mathcal{O}(\lambda^{\frac{1}{2\alpha}}) \rightarrow 0$, which implies h here has the magnitude $\mathcal{O}(\log^{-\frac{1}{2}}(n))$. In the following lemma, we will again start from a univariate case.

Lemma 13 *Given the equivalent kernel introduced above, we have $\tilde{\mathcal{O}}(\cdot)$ means $\mathcal{O}(\cdot)$ modulo poly-log terms):*

1. $\|\tilde{K}_\lambda\|_\infty \lesssim \sigma^{-d} h^{-d} = \tilde{\mathcal{O}}(\sigma^{-d})$;
2. *There exists some constant $C_3 > 0$ such that for $|\mathbf{j}| \leq d$,*

$$|D^{\mathbf{j}} \tilde{K}_\lambda(x, y)| \lesssim (\sigma h)^{-|\mathbf{j}|-d} e^{-C_3 |x-y| \sigma^{-1} h} = \tilde{\mathcal{O}}(\sigma^{-|\mathbf{j}|-d} e^{-C_3 |x-y| \sigma^{-1} h}).$$

Proof

Again we begin with univariate cases. From equation (13), we have

$$\|\tilde{K}_\lambda\|_\infty \leq \int_{-\infty}^{\infty} \frac{1}{1 + \frac{\lambda}{\sigma} e^{(\sigma s)^2}} ds \leq 2 \left[\int_0^{\sigma^{-1} h^{-1}} \frac{1}{1 + 0} ds + \int_{\sigma^{-1} h^{-1}}^{\infty} \frac{1}{\frac{\lambda}{\sigma} e^{(\sigma s)^2}} ds \right]$$

The integral is divided into two parts in which 1 and $\frac{\lambda}{\sigma} e^{(\sigma s)^2}$ dominate respectively. What's more, applying the property of error function that $\int_x^\infty e^{-t^2} dt = \mathcal{O}(\frac{e^{-x^2}}{x})$ (it holds when x is large enough), we can further obtain

$$\|\tilde{K}_\lambda\|_\infty \lesssim 2 \left[\sigma^{-1} h^{-1} + \frac{1}{\lambda} h e^{-h^{-2}} \right] \lesssim \sigma^{-1} h^{-1}$$

which is the first claimed property.

To prove the second one, we still apply the residue theorem to the following function ($|x - y|$ is denoted as $|u|$ for simplicity),

$$g(z) = \frac{e^{2\pi\sqrt{-1}|u|z}}{1 + \frac{\lambda}{\sigma} e^{(\sigma z)^2}}, \quad z \in \mathbb{C},$$

which is holomorphic on the complex plane except the roots $z_i, i \in \mathbb{Z}$ to the following equation:

$$1 + \frac{\lambda}{\sigma} e^{(\sigma z)^2} = 0$$

Therefore, z_{2k-1} and z_{2k} , for $k \in \mathbb{Z}$, are the two roots of the equation:

$$\sigma^2 z^2 = (h^{-2} + \sqrt{-1}(2k-1)\pi)$$

and $z_{2k-1} = -z_{2k}$. Without loss of generality, we assume $\text{Im}(z_{2k-1}) > 0$. Direct calculations roughly show that $|\text{Im}(z_{2k-1})| \gtrsim \sigma^{-1}$ and $|z_{2k-1}| \lesssim \sigma^{-1}$ for each $k \in \mathbb{Z}$. Further analysis would be provided later.

Note we could only focus on the case $|u| > \sigma h^{-1}$, since otherwise

$$|\tilde{K}_\lambda(u)| \leq C(\sigma h)^{-1} \leq C e^{C_3} (\sigma h)^{-1} e^{-C_3 |u| \sigma^{-1} h},$$

and the claimed property would be proved automatically. Now we apply the residue theorem to the following contour integral

$$\int_C g(z) dz = \int_C \frac{e^{2\pi\sqrt{-1}|u|z}}{1 + \frac{\lambda}{\sigma} e^{(\sigma z)^2}} dz,$$

where the contour C goes along the real line from $-R$ to R and then counter-clockwise along a semicircle centering at 0 from R to $-R$, for some sufficiently large constant $R > 0$. Denote the index set A_R as the set of all the indices k that the roots $\{z_{2k-1}\}_k$ are inside the contour C . The residue theorem implies

$$\int_C g(z) dz = 2\pi\sqrt{-1} \sum_{k \in A_R} \frac{e^{2\pi\sqrt{-1}|u|z_{2k-1}}}{2\sigma\lambda e^{(\sigma z_{2k-1})^2} z_{2k-1}},$$

Since $1 + \frac{\lambda}{\sigma} e^{(\sigma z)^2} = 0$, the above expression can be further simplified into

$$\int_C g(z) dz = -\pi\sqrt{-1} \sum_{k \in A_R} \frac{e^{2\pi\sqrt{-1}|u|z_{2k-1}}}{\sigma^2 z_{2k-1}}.$$

Note the set A_R is symmetric about 0 and goes to \mathbb{Z} as $R \rightarrow \infty$. We can first pair the opposite k and denote $z_{2k-1} = a_k + b_k\sqrt{-1}$, $z_{1-2k} = -a_k + b_k\sqrt{-1}$ for convenience. In this case,

$$\begin{aligned} & \frac{e^{2\pi\sqrt{-1}|u|z_{2k-1}}}{\sigma^2 z_{2k-1}} + \frac{e^{2\pi\sqrt{-1}|u|z_{1-2k}}}{\sigma^2 z_{1-2k}} = \frac{e^{-2\pi|u|b_k}}{-\sigma^2(a_k^2 + b_k^2)} 2\sqrt{-1}(b_k \cos(2\pi|u|a_k) - a_k \sin(2\pi|u|a_k)) \\ &= \frac{2\sqrt{-1}e^{-2\pi|u|b_k}}{-\sigma^2\sqrt{a_k^2 + b_k^2}} \cos(2\pi|u|a_k + \arctan(a_k/b_k)) \end{aligned}$$

And hence the sequence of the integral over the semicircle C with radius R would converge to

$$\frac{-2\pi}{\sigma^2} \sum_{k=1}^{\infty} \frac{e^{-2\pi|u|b_k}}{\sqrt{a_k^2 + b_k^2}} \cos(2\pi|u|a_k + \arctan(a_k/b_k)) \leq \frac{2\pi}{\sigma^2} \sum_{k=1}^{\infty} \frac{e^{-2\pi|u|b_k}}{\sqrt{a_k^2 + b_k^2}}$$

To further analyze the scale of the infinite series, we need to uncover the form of the coefficient a_k, b_k . Recall $z_{2k-1}^2 = \frac{1}{\sigma^2}(\ln \frac{\sigma}{\lambda} + (2k-1)\pi)$, and the corresponding derivation is,

$$\begin{aligned} a_k^2 + b_k^2 &= \sigma^{-2}(\ln^2 \frac{\sigma}{\lambda} + ((2k-1)\pi)^2)^{\frac{1}{2}} \\ 2b_k^2 &= (a_k^2 + b_k^2) - (a_k^2 - b_k^2) = \sigma^{-2} \left[(\ln^2 \frac{\sigma}{\lambda} + ((2k-1)\pi)^2)^{\frac{1}{2}} - (\ln \frac{\sigma}{\lambda}) \right] \\ &= \frac{\sigma^{-2}((2k-1)\pi)^2}{(\ln^2 \frac{\sigma}{\lambda} + ((2k-1)\pi)^2)^{\frac{1}{2}} + (\ln \frac{\sigma}{\lambda})} \end{aligned}$$

Denote $H \equiv (\frac{h^{-2}}{\pi} + 1)/2$. The curve of a_k, b_k could be roughly divided into two stages, $k \leq \lfloor H \rfloor$ and $k \geq \lceil H \rceil$. In the first stage, $a_k^2 + b_k^2 \geq \sigma^{-2} \ln \frac{\sigma}{\lambda} = (\sigma h)^{-2}$ and $2b_k^2 \geq$

$\sigma^{-2} \frac{((2k-1)\pi)^2}{2 \ln \frac{\sigma}{\lambda}} = \sigma^{-2} \frac{((2k-1)\pi)^2}{2h^{-2}}$; in the second stage, $a_k^2 + b_k^2 \geq \sqrt{2}\pi\sigma^{-2}(2k-1)$ and $2b_k^2 \geq \sigma^{-2} \frac{((2k-1)\pi)^2}{3\pi(2k-1)} = \sigma^{-2} \frac{(2k-1)\pi}{3}$. The infinite series could be therefore bounded as

$$\begin{aligned} \frac{2\pi}{\sigma^2} \sum_{k=1}^{\lfloor H \rfloor} \frac{e^{-2\pi|u|b_k}}{\sqrt{a_k^2 + b_k^2}} &\lesssim \sigma^{-1}h \sum_{k=1}^{\lfloor H \rfloor} e^{-C_3|u|\sigma^{-1}hk} \\ \frac{2\pi}{\sigma^2} \sum_{k=\lceil H \rceil}^{\infty} \frac{e^{-2\pi|u|b_k}}{\sqrt{a_k^2 + b_k^2}} &\lesssim \sigma^{-2} \sum_{k=\lceil H \rceil}^{\infty} \frac{e^{-C_3|u|\sigma^{-1}\sqrt{k}}}{\sigma^{-1}\sqrt{k}} \end{aligned}$$

The two series above will converge rapidly when n is large enough. The scale of the two series above will therefore depend on their own first terms. The first series would be bounded as a constant multiple of $\sigma^{-1}h \cdot h^{-2}e^{-C_3|u|\sigma^{-1}h \cdot 1} = (\sigma h)^{-1}e^{-C_3|u|(\sigma h)^{-1}}$; due to the decreasing sequence, the last series could be bounded in the following way (note $|u| > \sigma h^{-1}$),

$$\begin{aligned} \sigma^{-1} \sum_{k=\lceil H \rceil}^{\infty} \frac{e^{-C_3|u|\sigma^{-1}\sqrt{k}}}{\sqrt{k}} &\leq \sigma^{-1} \left[\frac{e^{-C_3|u|\sigma^{-1}\sqrt{\lceil H \rceil}}}{\sqrt{\lceil H \rceil}} + \int_{\lceil H \rceil}^{\infty} \frac{e^{-C_3|u|\sigma^{-1}\sqrt{x}}}{\sqrt{x}} dx \right] \\ &\leq \sigma^{-1} \left[h e^{-C_3|u|(\sigma h)^{-1}} + \frac{2\sigma}{C_3|u|} e^{-C_3|u|(\sigma h)^{-1}} \right] \lesssim \sigma^{-1} h e^{-C_3|u|(\sigma h)^{-1}} \end{aligned}$$

And hence the whole series would be bounded by $(\sigma h)^{-1}e^{-C_3|u|\sigma^{-1}h}$.

Then, we split the contour C into a straight part (real line) and a curved arc, so that

$$\int_C g(z) dz = \int_{(-R,R)} g(z) dz + \int_{\text{arc}} g(z) dz,$$

where the arc part satisfies $z = Re^{\sqrt{-1}\theta}$, $\theta \in [0, \pi]$ and hence,

$$\left| \int_{\text{arc}} g(z) dz \right| = \left| \int_0^\pi \frac{e^{2\pi\sqrt{-1}|u|Re^{\sqrt{-1}\theta}}}{1 + \frac{\lambda}{\sigma} e^{\sigma^2 R^2 e^{2\sqrt{-1}\theta}}} \sqrt{-1} R e^{\sqrt{-1}\theta} d\theta \right|$$

where the module of the integrand could be bounded by $\frac{e^{-2\pi|u|R \sin \theta}}{|1 - \frac{\lambda}{\sigma} e^{\sigma^2 R^2 \cos(2\theta)}}|$. By taking $R \rightarrow \infty$ and requiring $|u| > 0$, we could observe that when $\sin \theta$ is bounded away from 0 the integrand is exponentially decaying; when $\sin \theta$ is nearly zero $\cos 2\theta = 1 - 2\sin^2 \theta \gg 0$ and the integrand would also go to 0. That's to say, the whole integral $\int_{\text{arc}} g(z) dz \rightarrow 0$. Putting all pieces together, we finally reach

$$|\tilde{K}_\lambda(x-y)| = \int_{-\infty}^{\infty} \frac{e^{2\pi\sqrt{-1}s(x-y)}}{1 + \frac{\lambda}{\sigma} e^{(\sigma s)^2}} ds \lesssim \sigma^{-1} h e^{-C_3|u|\sigma^{-1}h} + \sigma^{-1} h^{-1} e^{-C_3|u|\sigma^{-1}h^{-1}},$$

which is part of the second desired property and similar to the conclusion in (12).

To complete the proof of the second property, we still need to bound the derivative of the equivalent kernel. Recall the differentiation property of Fourier transform, and $\mathcal{F}[\tilde{K}'_\lambda]$ could be written as:

$$\mathcal{F}[\tilde{K}'_\lambda] = \frac{2\pi\sqrt{-1}s}{1 + \frac{\lambda}{\sigma} e^{(\sigma s)^2}}.$$

With the expression above we can bound the sup norm of the derivative,

$$\|\tilde{K}'_\lambda\|_\infty \leq 4\pi \int_0^\infty \frac{s}{1 + \frac{\lambda}{\sigma} e^{(\sigma s)^2}} ds \leq 4\pi \left[\int_0^{\sigma^{-1}h^{-1}} \frac{s}{1+0} ds + \int_{\sigma^{-1}h^{-1}}^\infty \frac{s}{\frac{\lambda}{\sigma} e^{(\sigma s)^2}} ds \right].$$

The integral is divided into two parts in which 1 and $\frac{\lambda}{\sigma} e^{(\frac{s}{\sigma})^2}$ dominate respectively. We can further obtain

$$\|\tilde{K}'_\lambda\|_\infty \lesssim \left[(\sigma h)^{-2} + \frac{1}{2\lambda\sigma} e^{-h^{-2}} \right] \lesssim (\sigma h)^{-2}$$

To exactly analyze behavior of the derivative of equivalent kernels, we can accordingly reset function g as:

$$g(z) = \frac{e^{2\pi\sqrt{-1}|u|z} 2\pi\sqrt{-1}z}{1 + \frac{\lambda}{\sigma} e^{(\sigma z)^2}}, \quad z \in \mathbb{C},$$

and by the same procedure obtain the following inequality:

$$\begin{aligned} \int_C g(z) dz &= 2\pi^2 \sqrt{-1} \sum_{k \in A_R} \frac{e^{2\pi\sqrt{-1}|u|z_{2k-1}}}{\sigma^2} \\ &= \frac{2\pi^2}{\sigma^2} \sum_{k=1}^\infty (e^{2\pi\sqrt{-1}|u|(a_k+b_k\sqrt{-1})} + e^{2\pi\sqrt{-1}|u|(-a_k+b_k\sqrt{-1})}) \\ &= \frac{4\pi^2}{\sigma^2} \sum_{k=1}^\infty e^{-2\pi|u|b_k} (\cos(2\pi|u|a_k)) \leq \frac{4\pi^2}{\sigma^2} \sum_{k=1}^\infty e^{-2\pi|u|b_k}. \end{aligned}$$

We would only focus on the case $|u| > (\sigma/h)^{-1}$, since otherwise $|\tilde{K}'_\lambda(u)| \leq C(\sigma h)^{-2}$, which is bounded by $\leq C e^{C_3} (\sigma h)^{-2} e^{-C_3|u|\sigma^{-1}h}$, and the claimed property would be proved automatically. Due to the aforementioned division of the series, we have (note $|u| > (\sigma/h)^{-1}$),

$$\begin{aligned} \int_C g(z) dz &\leq \frac{4\pi^2}{\sigma^2} \left(\sum_{k=1}^{\lfloor H \rfloor} e^{-2\pi|u|b_k} + \sum_{k=\lceil H \rceil}^\infty e^{-2\pi|u|b_k} \right) \\ &\lesssim \frac{4\pi^2}{\sigma^2} \left[h^{-2} e^{-C_3|u|\sigma^{-1}h} + e^{-C_3|u|\sigma^{-1}h^{-1}} + \int_{k=\lceil H \rceil}^\infty e^{-C_3|u|\sigma^{-1}\sqrt{k}} dk \right] \\ &\lesssim \frac{1}{(\sigma h)^2} \left[e^{-C_3|u|\sigma^{-1}h} + \frac{2\sigma}{C_3|u|} \left(h^{-2} e^{-C_3|u|\sigma^{-1}h^{-1}} + \frac{\sigma}{C_3|u|} e^{-C_3|u|\sigma^{-1}h^{-1}} \right) \right] \\ &\lesssim \frac{1}{(\sigma h)^2} e^{-C_3|u|\sigma^{-1}h}. \end{aligned}$$

As for the integral over the arc part, its value is still negligible as

$$\left| \int_{\text{arc}} g(z) dz \right| \leq \left| \int_0^\pi \frac{e^{2\pi\sqrt{-1}|u|Re^{\sqrt{-1}\theta}} 2\pi\sqrt{-1}Re^{\sqrt{-1}\theta}}{1 + \frac{\lambda}{\sigma} e^{\sigma^2 R^2 e^{2\sqrt{-1}\theta}}} R d\theta \right|$$

where the module of the integrand could be bounded by $\frac{e^{-2\pi|u|R\sin\theta}2\pi R^2}{|1-\frac{\lambda}{\sigma}e^{\sigma^2 R^2\cos(2\theta)}|}$. The bound goes to 0 when $R \rightarrow \infty$ and $|u| > 0$ are assumed as before, and the integral over the arc is again negligible. Putting all pieces together, we finally reach

$$|\tilde{K}'_\lambda(x-y)| = \left| \int_{-\infty}^{\infty} \frac{e^{2\pi\sqrt{-1}s(x-y)}(2\pi\sqrt{-1}s)}{1 + \frac{\lambda}{\sigma}e^{(\sigma s)^2}} ds \right| \lesssim (\sigma h)^{-2} e^{-C_3|u|\sigma^{-1}h},$$

which completes the proof of the second property in univariate cases.

For multivariate cases, again by applying polar coordinate transformation, the original integral could be bounded as

$$\begin{aligned} \|\tilde{K}_\lambda\|_\infty &\lesssim \int_0^\infty \frac{r^{d-1}}{1 + \frac{\lambda}{\sigma^d}e^{(\sigma r)^2}} dr \leq \int_0^{\sigma^{-1}h^{-1}} \frac{r^{d-1}}{1+0} dr + \int_{\sigma^{-1}h^{-1}}^\infty \frac{r^{d-1}}{\frac{\lambda}{\sigma^d}e^{(\sigma r)^2}} dr \\ &\lesssim (\sigma h)^{-d} + \frac{1}{\lambda} \int_{h^{-1}}^\infty r^{d-1} e^{-r^2} dr \lesssim (\sigma h)^{-d} - \frac{1}{\lambda} \int_{h^{-1}}^\infty r^{d-2} de^{-r^2}. \end{aligned}$$

After repeatedly using integration by parts, the last term could be further bounded by $(\sigma h)^{-d} + \sigma^{-d}h^{-(d-2)}$, which validates the first claim in this lemma.

For the second claim, we would still use the same strategy, utilizing the isotropy and some other tricks, as in the proof for Matérn kernels. Specifically, we would focus on the special case

$$\left| \int_{\mathbb{R}^d} \frac{e^{2\pi\sqrt{-1}\|u\|s_1}}{1 + \frac{\lambda}{\sigma^d}e^{\sigma^2(\|s_{-1}\|^2 + s_1^2)}} \prod_{i=1}^d s_i^{\mathbf{j}_i} ds \right| \leq \int_{\mathbb{R}^{d-1}} \prod_{i=2}^d |s_i|^{\mathbf{j}_i} \cdot \left| \int_{-\infty}^\infty \frac{e^{2\pi\sqrt{-1}\|u\|s_1}|s_1|^{\mathbf{j}_1}}{1 + \frac{\lambda}{\sigma^d}e^{\sigma^2(\|s_{-1}\|^2 + s_1^2)}} ds_1 \right| ds_{-1},$$

and define $h^{-2} := \ln(\frac{\sigma^d}{\lambda})$, $t_s := |h^{-2} - \sigma^2\|s_{-1}\|^2|$, $\lambda \lesssim \sigma^d \lesssim h^{-d}$. Again we divide the integral into two different domains, $D_1 := \{\sigma^2\|s_{-1}\|^2 < h^{-2}\}$ and $D_2 := \{\sigma^2\|s_{-1}\|^2 \geq h^{-2}\}$. Moreover, we apply residue theorem to the internal integral and similarly have

$$\begin{aligned} \left| \int_{-\infty}^\infty \frac{e^{2\pi\sqrt{-1}\|u\|s_1}|s_1|^{\mathbf{j}_1}}{1 + \frac{\lambda}{\sigma^d}e^{\sigma^2(\|s_{-1}\|^2 + s_1^2)}} ds_1 \right| &= \left| 2\pi\sqrt{-1} \sum_{k=-\infty}^\infty \frac{e^{2\pi\sqrt{-1}\|u\|z_{2k-1}}(2\pi\sqrt{-1}z_{2k-1})^{\mathbf{j}_1}}{-2\sigma^2 z_{2k-1}} \right| \\ &\lesssim \sigma^{-2} \sum_{k=1}^\infty e^{2\pi\sqrt{-1}\|u\|z_{2k-1}} (z_{2k-1})^{\mathbf{j}_1-1}, \end{aligned}$$

where $z_{2k-1} = a_k + \sqrt{-1}b_k$, and

$$\begin{aligned} a_k^2 + b_k^2 &= \sigma^{-2}(t_s^2 + ((2k-1)\pi)^2)^{\frac{1}{2}} \\ 2b_k^2 &= (a_k^2 + b_k^2) - (a_k^2 - b_k^2) = \sigma^{-2} \left[(t_s^2 + ((2k-1)\pi)^2)^{\frac{1}{2}} - t_s \right] \\ &= \frac{\sigma^{-2}((2k-1)\pi)^2}{(t_s^2 + ((2k-1)\pi)^2)^{\frac{1}{2}} + t_s} \end{aligned}$$

We begin with the first domain D_1 , in which $\|s_{-1}\|^2 \leq (\sigma h)^{-2}$. We need to set a threshold $H = (\frac{t_s}{\pi} + 1)/2$ for the index k . When $k \leq \lfloor H \rfloor$, we have

$$\begin{aligned} 2b_k^2 &\geq \sigma^{-2} \frac{(2k-1)^2\pi^2}{3t_s} \Rightarrow b_k \gtrsim \sigma^{-1}\sqrt{t_s}^{-1}k \\ \sigma^{-2}t_s &\leq a_k^2 + b_k^2 \leq \sqrt{2}\sigma^{-2}t_s \Rightarrow |z_{2k-1}| = \Theta(\sigma^{-1}\sqrt{t_s}); \end{aligned}$$

when $k \geq \lceil H \rceil$, we have

$$\begin{aligned} 2b_k^2 &\geq \sigma^{-2} \frac{(2k-1)^2 \pi^2}{3(2k-1)\pi} \Rightarrow b_k \gtrsim \sigma^{-1} \sqrt{k} \\ \sigma^{-2}(2k-1)\pi &\leq a_k^2 + b_k^2 \leq \sqrt{2}\sigma^{-2}(2k-1)\pi \Rightarrow |z_{2k-1}| = \Theta(\sigma^{-1} \sqrt{k}); \end{aligned}$$

and the series would be bounded by

$$\begin{aligned} \sigma^{-2} \sum_{k=1}^{\lceil H \rceil} e^{-2\pi|u|b_k|z_{2k-1}|^{\mathbf{j}_1-1}} &\lesssim \sigma^{-2} (\sigma^{-1} \sqrt{t_s})^{\mathbf{j}_1-1} \sum_{k=1}^{\lceil H \rceil} e^{-C_3|u|\sigma^{-1} \sqrt{t_s}^{-1} k} \\ &\lesssim \sigma^{-(\mathbf{j}_1+1)} \sqrt{t_s}^{\mathbf{j}_1-1} e^{-C_3|u|\sigma^{-1} \sqrt{t_s}^{-1}} \\ \sigma^{-2} \sum_{k=\lceil H \rceil}^{\infty} e^{-2\pi|u|b_k|z_{2k-1}|^{\mathbf{j}_1-1}} &\lesssim \sigma^{-2} \sum_{k=\lceil H \rceil}^{\infty} e^{-C_3|u|\sigma^{-1} \sqrt{k}} (\sigma^{-1} \sqrt{k})^{\mathbf{j}_1-1} \\ &\lesssim \sigma^{-(\mathbf{j}_1+1)} (e^{-C_3|u|\sigma^{-1} \sqrt{\lceil H \rceil}} \sqrt{\lceil H \rceil}^{\mathbf{j}_1-1} \\ &\quad + \int_{\lceil H \rceil}^{\infty} e^{-C_3|u|\sigma^{-1} \sqrt{x}} \sqrt{x}^{\mathbf{j}_1-1} dx) \\ &\lesssim \sigma^{-(\mathbf{j}_1+1)} (e^{-C_3|u|\sigma^{-1} \sqrt{\lceil H \rceil}} \sqrt{\lceil H \rceil}^{\mathbf{j}_1-1} \\ &\quad + 1/(C_3|u|\sigma^{-1}) e^{-C_3|u|\sigma^{-1} \sqrt{\lceil H \rceil}} \sqrt{\lceil H \rceil}^{\mathbf{j}_1}) \\ &\lesssim \sigma^{-(\mathbf{j}_1+1)} \sqrt{\lceil H \rceil}^{\mathbf{j}_1-1} e^{-C_3|u|\sigma^{-1} \sqrt{\lceil H \rceil}}. \end{aligned}$$

We drop one term in the last line as $\sigma \sqrt{\lceil H \rceil} \leq \sigma h^{-1} \lesssim 1$, and note the first series would only appear when $t_s > \pi$, and $\lceil H \rceil = \Theta(\max(t_s/\pi, 1))$.

For the integral over the domain D_1 , it would be bounded as

$$\begin{aligned} &\int_{D_1} \frac{e^{2\pi\sqrt{-1}\|u\|s_1}}{1 + \frac{\lambda}{\sigma^d} e^{\sigma^2(\|s_{-1}\|^2 + s_1^2)}} \prod_{i=1}^d |s_i|^{\mathbf{j}_i} ds \\ &\leq \int_{\|s_{-1}\| \leq \frac{1}{\sigma h}} \prod_{i=2}^d |s_i|^{\mathbf{j}_i} \cdot \int_{-\infty}^{\infty} \frac{e^{2\pi\sqrt{-1}\|u\|s_1} |s_1|^{\mathbf{j}_1}}{1 + \frac{\lambda}{\sigma^d} e^{\sigma^2\|s_{-1}\|^2} e^{\sigma^2 s_1^2}} ds_1 ds_{-1} \\ &\lesssim \sigma^{-(\mathbf{j}_1+1)} \int_{\|s_{-1}\| \leq \frac{1}{\sigma h}} \|s_{-1}\|^{\mathbf{j}|\mathbf{j}_1-1} \cdot (\sqrt{t_s}^{\mathbf{j}_1-1} e^{-C_3|u|\sigma^{-1} \sqrt{t_s}^{-1}} + \sqrt{\lceil H \rceil}^{\mathbf{j}_1-1} e^{-C_3|u|\sigma^{-1} \sqrt{\lceil H \rceil}}) ds_{-1} \\ &\lesssim \sigma^{-(\mathbf{j}_1+1)} \left(\int_0^{\frac{1}{\sigma h}} r^{|\mathbf{j}|\mathbf{j}_1+d-2} \sqrt{t_s}^{\mathbf{j}_1-1} e^{-C_3|u|\sigma^{-1} \sqrt{t_s}^{-1}} dr \right. \\ &\quad \left. + \int_0^{\frac{1}{\sigma h}} r^{|\mathbf{j}|\mathbf{j}_1+d-2} \sqrt{\lceil H \rceil}^{\mathbf{j}_1-1} e^{-C_3|u|\sigma^{-1} \sqrt{\lceil H \rceil}} dr \right). \end{aligned}$$

To bound the first integral term, we should utilize a transformation $r = \frac{\sin(\theta)}{\sigma h}$, $t_s = h^{-1} \cos(\theta)$, and have

$$\begin{aligned} & \int_0^{\frac{1}{\sigma h}} r^{|\mathbf{j}| - \mathbf{j}_1 + d - 2} \sqrt{t_s}^{\mathbf{j}_1 - 1} e^{-C_3 |u| \sigma^{-1} \sqrt{t_s}^{-1}} dr \\ &= (\sigma h)^{-(|\mathbf{j}| - \mathbf{j}_1 + d - 2)} h^{-(\mathbf{j}_1 - 1)} \int_0^{\pi/2} \sin(\theta)^{|\mathbf{j}| - \mathbf{j}_1 + d - 2} \cos(\theta)^{\mathbf{j}_1 - 1} e^{-C_3 |u| \sigma^{-1} h / \cos(\theta)} d \frac{\sin(\theta)}{\sigma h} \\ &\leq (\sigma h)^{-(|\mathbf{j}| - \mathbf{j}_1 + d - 1)} h^{-(\mathbf{j}_1 - 1)} \int_0^{\pi/2} e^{-C_3 |u| \sigma^{-1} h} d\theta \lesssim \sigma^{-(|\mathbf{j}| - \mathbf{j}_1 + d - 1)} h^{-(|\mathbf{j}| + d - 2)} e^{-C_3 |u| \sigma^{-1} h}, \end{aligned}$$

the second integral term could be addressed by utilizing the fact $\lceil H \rceil \geq 1$

$$\begin{aligned} & \int_0^{\frac{1}{\sigma h}} r^{|\mathbf{j}| - \mathbf{j}_1 + d - 2} \sqrt{\lceil H \rceil}^{\mathbf{j}_1 - 1} e^{-C_3 |u| \sigma^{-1} \sqrt{\lceil H \rceil}} dr \\ &\leq \int_{\sigma^{-1}(h^{-2} - \pi)^{\frac{1}{2}}}^{\frac{1}{\sigma h}} r^{|\mathbf{j}| - \mathbf{j}_1 + d - 2} e^{-C_3 |u| \sigma^{-1}} dr + \int_0^{\frac{1}{\sigma h}} r^{|\mathbf{j}| - \mathbf{j}_1 + d - 2} \sqrt{t_s}^{\mathbf{j}_1 - 1} e^{-C_3 |u| \sigma^{-1}} dr \\ &\lesssim (\sigma h)^{-(|\mathbf{j}| - \mathbf{j}_1 + d - 1)} h^{-(\mathbf{j}_1 - 1)} e^{-C_3 |u| \sigma^{-1}} \int_0^{\pi/2} \sin(\theta)^{|\mathbf{j}| - \mathbf{j}_1 + d - 2} \cos(\theta)^{\mathbf{j}_1} d\theta \\ &\leq (\sigma h)^{-(|\mathbf{j}| - \mathbf{j}_1 + d - 1)} h^{-(\mathbf{j}_1 - 1)} e^{-C_3 |u| \sigma^{-1} h}, \end{aligned}$$

which could infer the total integral over domain D_1 should be $\mathcal{O}(\sigma^{-(|\mathbf{j}| + d)} h^{-(|\mathbf{j}| + d - 2)} e^{-C_3 |u| \sigma^{-1} h})$.

Over the second domain D_2 , we can similarly divide the series into two parts by the threshold H . We notice $\sqrt{t_s}$ and \sqrt{k} would respectively dominate the scale of b_k or $|z_{2k-1}|$ in the two parts, as

$$\begin{aligned} 2b_k^2 &\geq \sigma^{-2}((2k - 1)\pi + t_s) \\ a_k^2 + b_k^2 &= \Theta(\sigma^{-2}((2k - 1)\pi + t_s)). \end{aligned}$$

Using a similar derivation as above, the two parts would be correspondingly bounded by

$$\begin{aligned} \sigma^{-2} \sum_{k=1}^{\lceil H \rceil} e^{-2\pi |u| b_k} |z_{2k-1}|^{\mathbf{j}_1 - 1} &\lesssim \sigma^{-(\mathbf{j}_1 + 1)} \sqrt{t_s}^{\mathbf{j}_1 - 1} \lceil H \rceil e^{-C_3 |u| \sigma^{-1} \sqrt{t_s}} \\ \sigma^{-2} \sum_{k=\lceil H \rceil}^{\infty} e^{-2\pi |u| b_k} |z_{2k-1}|^{\mathbf{j}_1 - 1} &\lesssim \sigma^{-(\mathbf{j}_1 + 1)} \sqrt{\lceil H \rceil}^{\mathbf{j}_1 - 1} e^{-C_3 |u| \sigma^{-1} \sqrt{\lceil H \rceil}}. \end{aligned}$$

Since $\lceil H \rceil \gtrsim t_s$ and $\lceil H \rceil \geq 1$, the overall series could be bounded by a constant multiple of $\sigma^{-(\mathbf{j}_1 + 1)} \sqrt{\lceil H \rceil}^{\mathbf{j}_1 + 1} e^{-C_3 |u| \sigma^{-1} \sqrt{\lceil H \rceil}}$. Therefore, by polar coordinate transformation, the integral over D_2 would be reduced to the following one,

$$\begin{aligned} \int_{\frac{1}{\sigma h}}^{\infty} r^{|\mathbf{j}| - \mathbf{j}_1 + d - 2} \sqrt{\lceil H \rceil}^{\mathbf{j}_1 + 1} e^{-C_3 |u| \sigma^{-1} \sqrt{\lceil H \rceil}} dr &= \int_{\frac{1}{\sigma h}}^{\frac{2}{\sigma h}} r^{|\mathbf{j}| - \mathbf{j}_1 + d - 2} \sqrt{\lceil H \rceil}^{\mathbf{j}_1 + 1} e^{-C_3 |u| \sigma^{-1} \sqrt{\lceil H \rceil}} dr \\ &\quad + \int_{\frac{2}{\sigma h}}^{\infty} r^{|\mathbf{j}| - \mathbf{j}_1 + d - 2} \sqrt{\lceil H \rceil}^{\mathbf{j}_1 + 1} e^{-C_3 |u| \sigma^{-1} \sqrt{\lceil H \rceil}} dr, \end{aligned}$$

where we further divide the integral based on whether $t_s > h^{-2}$. For the first stage, utilizing $\lceil H \rceil \geq 1$, we can bound it as

$$\begin{aligned} \int_{\frac{1}{\sigma h}}^{\frac{2}{\sigma h}} r^{|\mathbf{j}| - \mathbf{j}_1 + d - 2} \sqrt{\lceil H \rceil}^{\mathbf{j}_1 + 1} e^{-C_3|u|\sigma^{-1}\sqrt{\lceil H \rceil}} dr &\lesssim \int_{\frac{1}{\sigma h}}^{\frac{2}{\sigma h}} r^{|\mathbf{j}| - \mathbf{j}_1 + d - 2} h^{-(\mathbf{j}_1 + 1)} e^{-C_3|u|\sigma^{-1}} dr \\ &\lesssim (\sigma h)^{-(|\mathbf{j}| - \mathbf{j}_1 + d - 1)} h^{-(\mathbf{j}_1 + 1)} e^{-C_3|u|\sigma^{-1}h}, \end{aligned}$$

for the second stage, we could apply $\lceil H \rceil = \Theta(\sigma^2 r^2)$, and have

$$\begin{aligned} \int_{\frac{2}{\sigma h}}^{\infty} r^{|\mathbf{j}| - \mathbf{j}_1 + d - 2} \sqrt{\lceil H \rceil}^{\mathbf{j}_1 + 1} e^{-C_3|u|\sigma^{-1}\sqrt{\lceil H \rceil}} dr &\lesssim \int_{\frac{2}{\sigma h}}^{\infty} r^{|\mathbf{j}| - \mathbf{j}_1 + d - 2} (\sigma r)^{\mathbf{j}_1 + 1} e^{-C_3|u|r} dr \\ &\lesssim \sigma^{\mathbf{j}_1 + 1} (\sigma h)^{-(|\mathbf{j}| + d - 1)} e^{-C_3|u|\sigma^{-1}h^{-1}}, \end{aligned}$$

which implies the scale of the integral over D_2 is $\mathcal{O}((\sigma h)^{-(|\mathbf{j}| + d)} e^{-C_3|u|\sigma^{-1}h})$. The second claim can thus be proved by simply combining the current results for D_1 and D_2 . ■

Appendix D. NUMERICAL INTEGRATION

To make the algorithm end in $\tilde{\mathcal{O}}(n)$ time, we need to efficiently compute all the leverage approximation (6) in the main paper. We first state an observation that the original multiple integral over \mathbb{R}^d could be simplified to a normal integral with only one variable. Then we propose a fast method to give the approximation of the integral, which only requires $\tilde{\mathcal{O}}(n)$ time to compute all the integrals.

D.1. Simplify the Integration by Polar Coordinate Transformation

An important feature of a Matérn kernel is the isotropy that the value of the kernel function $K_\alpha(x)$ only depends on the module $\|x\|_2$ (for simplicity $\|\cdot\|_2$ would be denoted as $\|\cdot\|$ from then on in this section). The property is shared by the corresponding spectral density $m_\alpha(s)$, and thus the Fourier transform of our rescaled leverage score approximation $\tilde{K}_\lambda(\cdot, t)$ also inherits the isotropy. In particular, given the center point t and a point x of interest, by Fourier transform formula,

$$\tilde{K}_\lambda(x, t) = \int_{\mathbb{R}^d} \mathcal{F}[\tilde{K}_\lambda(\cdot, t)](s) \exp(2\pi\sqrt{-1}x^T s) ds = \int_{\mathbb{R}^d} \frac{\exp(2\pi\sqrt{-1}(x - t)^T s)}{p(t) + \lambda/m_\alpha(s)} ds. \quad (14)$$

Considering the specific case $x = t$ in computing leverage score approximation, the value of the integrand would be the same for any s with the same module $\|s\|$. By polar coordinate transformation, we obtain

$$\tilde{K}_\lambda(t, t) = \int_0^\infty \frac{1}{p(t) + \lambda/m_\alpha(r)} \cdot S_{d-1}(r) dr$$

where $S_{d-1}(r)$ is the surface area of a (d) -dim ball with radius r .

It is worth mentioning for the general case $x \neq t$, the isotropy could also be utilized to accelerate the computation. In some geostatistics literature, for example, Hankel transform (Kleiber and Nychka, 2015) is applied to simplify the integration into a univariate integral for two-dimensional processes with Matérn kernels. We extend this idea to kernels with dimension more than two and represent the rescaled leverage score approximation $\tilde{K}_\lambda(x, t)$ as a double integral. We notice the value of the integrand in equation (14) would be the same for any s with the same module $\|s\|$ and the same inner product $(x-t)^T s$. Since the spectral density $m_\alpha(s)$ only depends on $\|s\|$, we slightly abuse the notation, instead representing it as $m_\alpha(\|s\|)$ to emphasize the isotropy. Moreover, by a certain coordinate transformation $r = \|s\|$, $\cos(\theta) = \frac{(x-t)^T s}{\|x-t\|\|s\|}$, we rewrite the integrand above as $\exp(2\pi\sqrt{-1}\|x-t\|r\cos(\theta))$, and observe that the integrand would remain unchanged with the input points from the intersection between the $(d-1)$ -sphere $\{s \in \mathbb{R}^d : \|s\| = r\}$ and the cone $\{s \in \mathbb{R}^d : (x-t)^T s = \|x-t\|\|s\|\cos(\theta)\}$ (the intersection is indeed a $(d-2)$ -sphere with radius $r\sin(\theta)$). With those notations, the original d -dim integral would thereby be calculated as

$$\tilde{K}_\lambda(x, t) = \int_0^\infty \int_0^\pi \frac{\exp(2\pi\sqrt{-1}\|x-t\|r\cos(\theta))}{p(t) + \lambda/m_\alpha(r)} \cdot S_{d-2}(r\sin(\theta)) r d\theta dr$$

where $S_{d-2}(r\sin(\theta))$ is the surface area of a $(d-1)$ -dim ball with radius $r\sin(\theta)$. The same trick applies to all the other stationary kernels with isotropic spectral density function, including Gaussian kernels.

D.2. Approximation of the Integrals

Directly, the integrals above can be computed by a reliable package QUADPACK with the specific integrator QAWF (Piessens et al., 2012), which is targeted at Fourier cosine transform. However, the computation is time-consuming, as QAWF implements an adaptive method so that when $\lambda \rightarrow 0$ it will require more function evaluations. To overcome the potential drawback, we propose a fast method to approximate the integration with $o(1)$ relative error in near-constant time.

For Matérn kernels, we would focus on the following integral of a simplified form,

$$\int_0^\infty \frac{x^{d-1}}{p + \lambda(1+x^2)^\alpha} dx.$$

Inspired by the derivation of the scale of the integral $O(\lambda^{-\frac{d}{2\alpha}})$, we rewrite the integral as

$$\int_0^\infty \frac{x^{d-1}}{p + (\lambda^{\frac{1}{\alpha}} + (\lambda^{\frac{1}{2\alpha}}x)^2)^\alpha} dx = \lambda^{-\frac{d}{2\alpha}} \int_0^\infty \frac{x^{d-1}}{p + (\lambda^{\frac{1}{\alpha}} + x^2)^\alpha} dx,$$

and intuitively want to replace $(\lambda^{\frac{1}{\alpha}} + x^2)$ with x^2 . We would show the approximation would only result in a small relative error of order $\mathcal{O}(\lambda^{\frac{1}{\alpha}}) = o(1)$ as required.

The difference between the two integrands is

$$\lambda^{-\frac{d}{2\alpha}} \left(\frac{x^{d-1}}{p + x^{2\alpha}} - \frac{x^{d-1}}{p + (\lambda^{\frac{1}{\alpha}} + x^2)^\alpha} \right) = \lambda^{-\frac{1}{2\alpha}} x^{d-1} \frac{(\lambda^{\frac{1}{\alpha}} + x^2)^\alpha - x^{2\alpha}}{(p + x^{2\alpha})(p + (\lambda^{\frac{1}{\alpha}} + x^2)^\alpha)}.$$

When $x^2 \leq \lambda^{\frac{1}{\alpha}}$, the numerator above would be bounded by $(2^\alpha - 1)\lambda$, and further we have

$$\frac{(\lambda^{\frac{1}{\alpha}} + x^2)^\alpha - x^{2\alpha}}{(p + x^{2\alpha})(p + (\lambda^{\frac{1}{\alpha}} + x^2)^\alpha)} \leq \frac{(2^\alpha - 1)\lambda}{(p + x^{2\alpha})(p + (\lambda^{\frac{1}{\alpha}} + x^2)^\alpha)} \lesssim \frac{\lambda^{\frac{1}{\alpha}}}{p + x^{2\alpha}}.$$

When $x^2 > \lambda^{\frac{1}{\alpha}}$, we can control the numerator by the first order Taylor approximation,

$$\frac{(\lambda^{\frac{1}{\alpha}} + x^2)^\alpha - x^{2\alpha}}{(p + x^{2\alpha})(p + (\lambda^{\frac{1}{\alpha}} + x^2)^\alpha)} \lesssim \frac{\lambda^{\frac{1}{\alpha}}(x^2)^{\alpha-1}}{(p + x^{2\alpha})(p + (\lambda^{\frac{1}{\alpha}} + x^2)^\alpha)} \lesssim \frac{\lambda^{\frac{1}{\alpha}}}{p + x^{2\alpha}},$$

where the last relation holds as $(x^2)^{\alpha-1} \lesssim p + (\lambda^{\frac{1}{\alpha}} + x^2)^\alpha$.

Then the total difference between two integrals would be bounded by a constant multiple of

$$\lambda^{-\frac{d}{2\alpha}} \int_0^\infty \frac{\lambda^{\frac{1}{\alpha}} x^{d-1}}{p + x^{2\alpha}} dx,$$

which is $O(\lambda^{-\frac{d}{2\alpha}} \lambda^{\frac{1}{\alpha}})$. Considering the magnitude of the original integral is $\Theta(\lambda^{-\frac{d}{2\alpha}})$, our claim regarding the relative error is validated.

We utilize the formula $\int_0^\infty \frac{dx}{1+x^a} = \frac{\pi/a}{\sin \pi/a}$ to give the final approximation:

$$\int_0^\infty \frac{x^{d-1}}{p + \lambda(1+x^2)^\alpha} dx \approx p^{\frac{d}{2\alpha}-1} \lambda^{-\frac{d}{2\alpha}} \frac{\pi/\frac{d}{2\alpha}}{\sin \pi/\frac{d}{2\alpha}}.$$

As the sampling probability is computed as the normalized leverage, we can even directly use $p^{\frac{d}{2\alpha}-1}$ as the rescaled leverage and ignore the rest factor.

For Gaussian kernels, the formula would be even easier, since there is a closed form expression for the target integral,

$$\frac{2}{\Gamma(d/2)} \int_0^\infty \frac{t^{d-1}}{p(2\pi\sigma^2)^{d/2} + \lambda e^{t^2}} dt = -\frac{Li_{d/2}(-\frac{p(2\pi\sigma^2)^{d/2}}{\lambda})}{p(2\pi\sigma^2)^{d/2}}$$

where σ is the bandwidth of the Gaussian kernel used, and $Li_{d/2}(\cdot)$ is the polylogarithm function with order $\frac{d}{2}$. The fast computation of the polylogarithm function has already been thoroughly studied by some previous works (Crandall, 2006; Vepřtas, 2008; Johansson, 2015), and they proposed various methods to compute $Li_{d/2}(c)$ with $\Theta(\log \log n)$ bits of precision ($\Theta(\frac{1}{\log n})$ relative error) and a polynomial of $\log \log n$ time. The total time to compute the leverage would thus still be $\tilde{O}(n)$.

Appendix E. DENSITY ESTIMATION

As we described in the main paper, by utilizing the distributional information, leverage scores in a KRR problem could be efficiently approximated by our analytical method. In the case we do not have prior knowledge of the distribution, we propose to estimate densities of data points via kernel density estimation, which have been discussed in the main paper

that by using some recent KDE methods with a sub-optimal error rate, we can perform the density estimation within $\tilde{O}(n)$ time. To further justify the usage of kernel density estimation, we imply by the following lemma that given an $o(1)$ error in KDE, the particular error in approximating statistical leverage scores due to the density estimation is asymptotically negligible.

Lemma 14 *Under the same assumptions before, $\forall x \in \text{spt}(p)$ (the support of p), given a fixed point t , the supremum of the error caused by the density estimate $\hat{p}(t)$ on point t , is bounded by a constant multiple of $h^{-d}|p(t) - \hat{p}(t)|$.*

Proof For simplicity, we first denote the leverage score approximation with estimated density as $\hat{\tilde{K}}_\lambda(x, x_i)$. Inserting the density estimation \hat{p} into the formula of rescaled leverage scores (equation 7 in the main paper), we obtain $\mathcal{F}[\hat{\tilde{K}}_\lambda(\cdot, x_i)](s) = \frac{e^{-2\pi\sqrt{-1}\langle x_i, s \rangle}}{\hat{p}(x_i) + \lambda(m_\alpha(s))^{-1}}$.

By triangle inequality, the supremum of the total error $|\hat{\tilde{K}}_\lambda(x, x_i) - G(x, x_i)|$ could be divided into two sources, one due to density estimation $|\hat{\tilde{K}}_\lambda(x, x_i) - \tilde{K}_\lambda(x, x_i)|$ and the other due to approximation error $|\tilde{K}_\lambda(x, x_i) - G_\lambda(x, x_i)|$, which has been thoroughly discussed in the appendix. Here we focus on the first term.

$$\begin{aligned} & \sup_{x \in \mathbb{R}^d} |\hat{\tilde{K}}_\lambda(x, x_i) - \tilde{K}_\lambda(x, x_i)| \\ &= \sup_{x \in \mathbb{R}^d} \left| \mathcal{F}^{-1}[\mathcal{F}[\hat{\tilde{K}}_\lambda(\cdot, x_i)]](x) - \mathcal{F}^{-1}[\mathcal{F}[\tilde{K}_\lambda(\cdot, x_i)]](x) \right| \\ &= \sup_{x \in \mathbb{R}^d} \left| \mathcal{F}^{-1} \left[\frac{|\hat{p}(x_i) - p(x_i)| e^{-2\pi\sqrt{-1}\langle x_i, s \rangle}}{(\hat{p}(x_i) + \lambda \cdot (m_\alpha(s))^{-1})(p(x_i) + \lambda \cdot (m_\alpha(s))^{-1})} \right](x) \right| \end{aligned}$$

$|\hat{p}(x_i) - p(x_i)|$ could be extracted as a factor, and we solely need to deal with the rest term

$$\begin{aligned} & \sup_{x \in \mathbb{R}^d} \left| \mathcal{F}^{-1} \left[\frac{e^{-2\pi\sqrt{-1}\langle x_i, s \rangle}}{(\hat{p}(x_i) + \lambda \cdot (m_\alpha(s))^{-1})(p(x_i) + \lambda \cdot (m_\alpha(s))^{-1})} \right](x) \right| \\ &= \sup_{x \in \mathbb{R}^d} \left| \int_{\mathbb{R}^d} \left[\frac{e^{-2\pi\sqrt{-1}\langle x_i - x, s \rangle}}{(\hat{p}(x_i) + \lambda \cdot (m_\alpha(s))^{-1})(p(x_i) + \lambda \cdot (m_\alpha(s))^{-1})} \right] ds \right| \end{aligned}$$

Relaxing the exponential term as 1 and using Cauchy-Schwarz inequality, we obtain

$$\begin{aligned} & \left| \int_{\mathbb{R}^d} \left[\frac{e^{-2\pi\sqrt{-1}\langle x_i - x, s \rangle}}{(\hat{p}(x_i) + \lambda \cdot (m_\alpha(s))^{-1})(p(x_i) + \lambda \cdot (m_\alpha(s))^{-1})} \right] ds \right| \\ & \leq \left| \int_{\mathbb{R}^d} \left[\frac{1}{(\hat{p}(x_i) + \lambda \cdot (m_\alpha(s))^{-1})(p(x_i) + \lambda \cdot (m_\alpha(s))^{-1})} \right] ds \right| \\ & \leq \left\| \frac{1}{\hat{p}(x_i) + \lambda \cdot (m_\alpha(s))^{-1}} \right\|_2 \cdot \left\| \frac{1}{p(x_i) + \lambda \cdot (m_\alpha(s))^{-1}} \right\|_2 \\ & \lesssim h^{-d/2} h^{-d/2} = h^{-d} \end{aligned}$$

The last inequality can be verified by Lemma 12. ■

We finally remark that given the $o(1)$ factor $|\hat{p}(x_i) - p(x_i)|$, the error $|\hat{\tilde{K}}_\lambda(x, x_i) - \tilde{K}_\lambda(x, x_i)|$ caused by the density estimation would therefore be $o(h^{-d})$, and thus is enough to make the relative error of leverage approximation vanish.

E.1. Missing assumptions for modified HBE

We list some advanced KDE methods in the main paper to show theoretically we can estimate the density with time complexity at most polynomial in the dimension d . Among them, modified Hashing-Based Estimators (HBE) (Backurs et al., 2019) is the most recent one. Taking this method as a representative, we copy the assumption in modified HBE here for the sake of completeness.

Assumption 15 ($(\frac{1}{2}, M)$ -LSHable) *Let $\mathcal{K}_e(x, y)$ be the kernel function used for KDE, for which there exists a distribution H of hash functions and $M \geq 1$ such that for every $x, y \in \mathbb{R}^d$,*

$$M^{-1} \cdot \mathcal{K}_e(x, y)^{\frac{1}{2}} \leq \mathbb{P}_{h \sim H} \{h(x) = h(y)\} \leq M \cdot \mathcal{K}_e(x, y)^{\frac{1}{2}}.$$

To attain the fast rate claimed by modified HBE, the core assumption above that the kernel used for KDE is $(\frac{1}{2}, M)$ -LSHable for some constant M is necessary. The authors have proved that some common kernels, such as Laplacian and exponential kernels, are $(\frac{1}{2}, \mathcal{O}(1))$ -LSHable; and thus a density estimator based on those kernels can be efficiently approximated by modified HBE.

Appendix F. TECHNICAL RESULTS

Some tricks in multivariate integrals are heavily utilized in this work, and here we present a lemma to address the technical details about it. We first would like to mention the notation $\int_{\mathbb{R}^d} f(x) dF_n(x)$ in our paper is not strict in general, as the multivariate version Riemann–Stieltjes integral is not well defined. In this appendix we just abuse the integral $\int_{\mathbb{R}^d} f(x) dF_n(x)$ to represent the summation $\frac{1}{n} \sum_{i=1}^n f(x_i)$, and the integral $\int_{\mathbb{R}^d} f(x) dF(x)$ to represent the expectation $\int_{\mathbb{R}^d} f(x) p(x) dx$.

The lemma is presented as follows. (cf. Section A.3 for the notations in the lemma.)

Lemma 16 (Multivariate integration by parts) *Given the absolute continuous approximation F with the compact support Ω and L_∞ density p , the empirical distribution F_n , and an integrand $g(\cdot) \in W^{\alpha, 2}$ independent of F_n , the certain integral of interest $\int_{C(y, \delta)} g(x) d(F_n - F)(x)$ is almost surely (considering the samples in F_n are drawn from F) equal to*

$$\sum_{\mathbf{A} \sqcup \mathbf{B} \sqcup \mathbf{C} = [d]} (-1)^{|\mathbf{A}| + |\mathbf{B}|} \int_{C(y_{\mathbf{A}}, \delta)} D^{\mathbf{I}_{\mathbf{A}}} g(x_{\mathbf{A}}; (y + \delta \cdot (-I_{\mathbf{B}} + I_{\mathbf{C}}))_{\mathbf{B} \sqcup \mathbf{C}}) \cdot (F_n - F)(x_{\mathbf{A}}; (y + \delta \cdot (-I_{\mathbf{B}} + I_{\mathbf{C}}))_{\mathbf{B} \sqcup \mathbf{C}}) dx_{\mathbf{A}},$$

where \sqcup is the notation for disjoint union. The sets \mathbf{B} and \mathbf{C} indeed indicate the certain dimensions to which lower and upper limits are assigned separately. Specifically, if $C(x_0, \delta) = \mathbb{R}^d$ ($\delta = \infty$) and $g(x)$ vanishes at infinity, $\int_{\mathbb{R}^d} g(x) d(F_n - F)(x) = (-1)^d \int_{\mathbb{R}^d} (F_n - F)(x) \frac{\partial^d g(x)}{\partial x_1 \partial x_2 \dots \partial x_d} dx$; if $g(x)$ and its mixed derivative (up to order α) vanish at infinity and are L -Lipschitz, the claim would hold without the assumption on the independence between g and F_n .

Proof Without loss of generality, we would illustrate our claim by a special 2-d case to avoid the tedious calculation. We would first prove the conclusion for an indefinitely differentiable density $p_{n,\epsilon}(x) = \frac{1}{n} \sum_{i=1}^n \eta_\epsilon(x - x_i)$, where the heat kernel $\eta_\epsilon(x) := \frac{1}{\sqrt{2\pi\epsilon}} \exp(-\frac{\langle x, x \rangle}{2\epsilon})$ of the Dirac delta function. (From then on in this proof, x_i means the i -th element of the vector x .) As a sketch of the proof, we would first show the lemma holds for the integral $\int_{C(y,\delta)} g(x)(p_{n,\epsilon}(x) - p(x))dx$, and finally prove as $\epsilon \rightarrow 0$, the integral would converge to the claimed expression in this lemma.

For simplicity, we denote $q(x) = p_{n,\epsilon}(x) - p(x)$ and $Q(x)$ is the corresponding distribution function. We further denote $Q_1(x_1; x_2) := \int_{-\infty}^{x_1} q(t, x_2)dt$ as a 1-d distribution function with a parameter x_2 , so that Riemann–Stieltjes integral is applicable to $Q_1(x_1; x_2)$. By definition $\int_{-\infty}^{x_2} Q_1(x_1; t)dt = Q(x_1, x_2)$, and with that we have

$$\begin{aligned} \int_{C(y,\delta)} g(x)q(x)dx &= \int_{y_2-\delta}^{y_2+\delta} \int_{y_1-\delta}^{y_1+\delta} g(x_1, x_2)q(x_1, x_2)dx_1dx_2 \\ &= \int_{y_2-\delta}^{y_2+\delta} \int_{y_1-\delta}^{y_1+\delta} g(x_1, x_2)dQ_1(x_1; x_2)dx_2 \end{aligned}$$

We can safely apply integration by parts to the inside integral and obtain:

$$\begin{aligned} \int_{C(y,\delta)} g(x)q(x)dx &= \int_{y_2-\delta}^{y_2+\delta} \left(g(x_1, x_2)Q_1(x_1; x_2) \Big|_{y_1-\delta}^{y_1+\delta} - \int_{y_1-\delta}^{y_1+\delta} Q_1 \frac{\partial g}{\partial x_1} dx_1 \right) dx_2 \quad (15) \\ &= \int_{y_2-\delta}^{y_2+\delta} g(y_1 + \delta, x_2)Q_1(y_1 + \delta, x_2) - g(y_1 - \delta, x_2)Q_1(y_1 - \delta, x_2)dx_2 - \int_{C(y,\delta)} Q_1 \frac{\partial g}{\partial x_1} dx. \end{aligned} \quad (16)$$

Now we expand the original integral into three terms. By repeatedly applying integration by parts to the first two terms, we have:

$$\begin{aligned} \int_{y_2-\delta}^{y_2+\delta} g(y_1 + \delta, x_2)Q_1(y_1 + \delta, x_2)dx_2 &= g(y_1 + \delta, y_2 + \delta)Q(y_1 + \delta, y_2 + \delta) \\ &\quad - g(y_1 + \delta, y_2 - \delta)Q(y_1 + \delta, y_2 - \delta) - \int_{y_2-\delta}^{y_2+\delta} Q_1(y_1 + \delta, x_2) \frac{\partial g(y_1 + \delta, x_2)}{\partial x_2} dx_2 \\ \int_{y_2-\delta}^{y_2+\delta} -g(y_1 - \delta, x_2)Q_1(y_1 - \delta, x_2)dx_2 &= -g(y_1 - \delta, y_2 + \delta)Q(y_1 - \delta, y_2 + \delta) \\ &\quad + g(y_1 - \delta, y_2 - \delta)Q(y_1 - \delta, y_2 - \delta) + \int_{y_2-\delta}^{y_2+\delta} Q_1(y_1 - \delta, x_2) \frac{\partial g(y_1 - \delta, x_2)}{\partial x_2} dx_2 \end{aligned}$$

For the last term, we need to change the order of integration and have,

$$\begin{aligned} & - \int_{C(y,\delta)} Q_1 \frac{\partial g}{\partial x_1} dx \\ &= - \int_{y_1-\delta}^{y_1+\delta} \int_{y_2-\delta}^{y_2+\delta} \frac{\partial g(x_1, x_2)}{\partial x_1} dQ(x_1, x_2)dx_1 = - \int_{y_1-\delta}^{y_1+\delta} Q(x_1, y_2 + \delta) \frac{\partial g(x_1, y_2 + \delta)}{\partial x_1} dx_1 \\ &\quad + \int_{y_1-\delta}^{y_1+\delta} Q(x_1, y_2 - \delta) \frac{\partial g(x_1, y_2 - \delta)}{\partial x_1} dx_1 + \int_{C(y,\delta)} Q \frac{\partial^2 g}{\partial x_1 \partial x_2} dx \end{aligned}$$

Summing up all the nine terms above, we would exactly obtain the claimed equation in the lemma. In particular, if $C(y, \delta) = \mathbb{R}^d$ ($\delta = \infty$) and $g(x)$ vanishes at infinity, the first two terms in equation (16) would be dropped, and finally the only term left is $\int_{\mathbb{R}^d} g(x)q(x)dx$, which is equal to $(-1)^d \int_{\mathbb{R}^d} Q(x) \frac{\partial^d g(x)}{\partial x_1 \partial x_2 \dots \partial x_d} dx$ as claimed.

To complete the proof, we still need to show the convergence. We would begin with the assumption $g(\cdot)$ belongs to a dense subset $\mathcal{D} \subset W^{\alpha,2}$, where \mathcal{D} is the space of test functions. Here we simply borrow some definitions and notations from the book (Debnath et al., 2005, Chapter 6), with respect to test functions and weak distributional convergence. A test function is defined as an infinitely differentiable function on \mathbb{R}^d vanishing outside of some bounded set. We denote weak distributional convergence for a sequence of distributions (P_m) to P as $P_m \rightarrow P$ if $\langle P_m, g \rangle \rightarrow \langle P, g \rangle, \forall g \in \mathcal{D}$. We can see our choice $P_{n,\epsilon} \rightarrow F_n$ in the weak distributional sense by setting $P_m = P_{n,1/m}$, and thus for the left hand side of our claim, $\int_{C(y,\delta)} g(x)d(P_{n,1/m} - F_n)(x) \rightarrow \int_{C(y,\delta)} g(x)d(F_n - F)(x)$ by some standard techniques; For the terms in the right hand side, we would illustrate by taking $\int_{C(y,\delta)} D^{\mathbf{I}^{[d]}} g(x)(P_{n,\epsilon} - P)(x)dx$ as an example. We note $D^{\mathbf{I}^{\mathbf{A}}} g$ is still a test function, and $P_{n,\epsilon}$ converges to F_n in L_2 , so that by Cauchy-Schwartz inequality we could obtain,

$$\begin{aligned} & \left| \int_{C(y,\delta)} D^{\mathbf{I}^{[d]}} g(x)(P_{n,\epsilon} - F_n)(x)dx \right| \\ & \leq \left(\int_{C(y,\delta)} |D^{\mathbf{I}^{[d]}} g(x)|^2 dx \cdot \int_{C(y,\delta)} |(P_{n,\epsilon} - F_n)(x)|^2 dx \right)^{\frac{1}{2}} \rightarrow 0, \end{aligned}$$

which implies our desired convergence.

The next step is to extend test functions to functions in $W^{\alpha,2}$. An important fact is that \mathcal{D} is a dense subspace of $W^{\alpha,2}$, and we can find a sequence of test functions converging to g in $W^{\alpha,2}$ and further a subsequence (g_m) converging to g both in $W^{\alpha,2}$ and almost everywhere, since convergence in $W^{\alpha,2}$ implies convergence in L_2 . The Cauchy-Schwartz inequality trick for the right hand side would still work as this time the L_2 norm of $D^{\mathbf{I}^{[d]}}(g(x) - g_m(x))$ goes to zero. For the left-hand side, as we assume the n samples are drawn from the absolutely continuous distribution F , for the certain sequence above we can show

$$\begin{aligned} \left| \int_{C(y,\delta)} (g(x) - g_m(x))dF(x) \right| & \leq \int_{C(y,\delta)} |g(x) - g_m(x)|p(x)dx \\ & \leq \|g(x) - g_m(x)\|_{1,\Omega} \cdot \|p\|_{\infty} \\ & \leq |\Omega|^{\frac{1}{2}} \|p\|_{\infty} \|g(x) - g_m(x)\|_2 \rightarrow 0, \end{aligned}$$

and with probability one, over the n sample points g_m would pointwisely go to g . We can thus conclude our claim would hold for functions in $W^{\alpha,2}$ almost surely.

Finally, for the special case in which $g(x)$ and its mixed derivative (up to order α) are L -Lipschitz, we are able to construct a convergent test function sequence g_m which would pointwisely converge to g over the compact support Ω containing all the samples in F_n . We first introduce a sequence of test functions

$$\phi_m := \begin{cases} \frac{m^{\frac{d(d+1)}{2}}}{\varphi} e^{(m^{\frac{d+1}{2}} \|x\|^2 - 1)^{-1}}, & \text{if } \|x\| < m^{-\frac{d+1}{2}}, \\ 0, & \text{otherwise,} \end{cases}$$

where $\varphi = \int \phi_1(x)dx$ is the normalization factor. The sequence $\{g_m\}$ is constructed as $\{\phi_m * (g \cdot 1_{m\Omega})\}$, the convolution of the test function ϕ_m and the truncation $g \cdot 1_{m\Omega}$, which is still a sequence of test functions. It can be shown the sequence g_m would go to g in $W^{\alpha,2}$. To validate it, we need to observe the fact that for $x \in m\Omega$,

$$\begin{aligned} |g_m(x) - g(x)| &= \left| \int \phi_m(t)(g(x-t) - g(x))dt \right| \leq \int_{t < m^{-\frac{d+1}{2}}} \phi_m(t)|g(x-t) - g(x)|dt \\ &\leq \frac{L}{m^{\frac{d+1}{2}}} \int_{t < m^{-\frac{d+1}{2}}} \phi_m(t)dt = \frac{L}{m^{\frac{d+1}{2}}}, \end{aligned}$$

where the second inequality holds because of the Lipschitz continuity. Therefore,

$$\begin{aligned} \int |g_m(x) - g(x)|^2 dx &= \int_{m\Omega} |g_m(x) - g(x)|^2 dx + \int_{\mathbb{R}^d - m\Omega} |g_m(x) - g(x)|^2 dx \\ &\leq \frac{L^2}{m^{d+1}} |m\Omega| + 2 \int_{\mathbb{R}^d - m\Omega} g^2(x) dx + 2 \int_{\mathbb{R}^d - m\Omega} g_m^2(x) dx. \end{aligned}$$

Note the first term is proportional to $1/m$, and $g(x)$ vanishes at infinity. The first two terms would both go to zero as $m \rightarrow \infty$. For the last term, we could utilize Jensen's inequality and have $g_m^2(x) \leq \int \phi_m(t)g^2(x-t)1_{m\Omega}(x-t)dt \leq \int \phi_m(t)g^2(x-t)dt$. Then,

$$\begin{aligned} \int_{\mathbb{R}^d - m\Omega} g_m^2(x) dx &\leq \int_{\mathbb{R}^d - m\Omega} \int_{\mathbb{R}^d} \phi_m(t)g^2(x-t)dt dx = \int_{\mathbb{R}^d} \phi_m(t) \int_{\mathbb{R}^d - m\Omega} g^2(x-t)dx dt \\ &\leq \int_{\mathbb{R}^d} \phi_m(t) \int_{(\mathbb{R}^d - m\Omega) + B(m^{-\frac{d+1}{2}})} g^2(x)dx dt \\ &= \int_{(\mathbb{R}^d - m\Omega) + B(m^{-\frac{d+1}{2}})} g^2(x)dx \rightarrow 0 \end{aligned}$$

where $B(m^{-\frac{d+1}{2}})$ is a ball with radius $m^{-\frac{d+1}{2}}$, and the last convergence holds again since $g(x)$ vanishes at infinity. Combining the pieces above, we can see $g_m \rightarrow g$ in L_2 and the similar conclusion holds for all its mixed derivatives up to order α , which means $g_m \rightarrow g$ in $W^{\alpha,2}$. In that case, the convergence for the right-hand side of our claim would still hold as in the paragraph above. For the left hand side, this time g_m would uniformly converge to g over Ω , and we can show the integral $\int_{C(y,\delta)} g_m(x)d(F_n - F)(x)$ would converge to $\int_{C(y,\delta)} g(x)d(F_n - F)(x)$, even if g depends on the empirical distribution F_n . ■